LABORATORY INVESTIGATION OF HYDRAULIC EFFICIENCY OF
TRANSVERSE GRATES IN ROADS

A THESIS SUBMITTED TO
THE GRADUATE SCHOOL OF NATURAL AND APPLIED SCIENCES
OF
MIDDLE EAST TECHNICAL UNIVERSITY

BY

CUMHUR ÖZBEY

IN PARTIAL FULFILLMENT OF THE REQUIREMENTS
FOR
THE DEGREE OF MASTER OF SCIENCE
IN
CIVIL ENGINEERING

DECEMBER 2015

Approval of the thesis:

LABORATORY INVESTIGATION OF HYDRAULIC EFFICIENCY OF TRANSVERSE GRATES IN ROADS

submitted by **CUMHUR ÖZBEY** in partial fulfillment of the requirements for the **degree of Master Science in Civil Engineering Department, Middle East Technical University** by,

Prof. Dr. Gülbin Dural Ünver
Dean, Graduate School of **Natural and Applied Sciences** _____

Prof. Dr. Ahmet Cevdet Yalçıner
Head of Department, **Civil Engineering** _____

Assoc. Prof. Dr. Şahnaz Tiğrek
Supervisor, **Civil Engineering Dept., Batman University** _____

Examining Committee Members

Prof. Dr. A. Melih Yanmaz
Civil Engineering Dept., METU _____

Assoc. Prof. Dr. Şahnaz Tiğrek
Civil Engineering Dept., Batman University _____

Prof. Dr. A. Burcu Altan Sakarya
Civil Engineering Dept., METU _____

Assoc. Prof. Dr. Mete Köken
Civil Engineering Dept., METU _____

Assist. Prof. Dr. Aslı Numanoğlu Genç
Civil Engineering Dept., Atılım University _____

Date: December 2015

I hereby declare that all information in this document has been obtained and presented in accordance with academic rules and ethical conduct. I also declare that, as required by these rules and conduct, I have fully cited and referenced all material and results that are not original to this work.

Name, Last name: Cumhur ÖZBEY

Signature :

ABSTRACT

LABORATORY INVESTIGATION OF HYDRAULIC EFFICIENCY OF TRANSVERSE GRATES IN ROADS

Özbey, Cumhur

M.S. Department of Civil Engineering

Supervisor: Assoc. Prof. Dr. Şahnaz Tiğrek

December 2015, 84 Pages

In this study, hydraulic efficiency of transverse grated inlet systems to be used in small roads is experimentally investigated. For this purpose, an existing experimental setup in the Hydromechanics Laboratory of METU is utilized. Three sets of experiments are conducted in order to examine the relationship between the total flow rate and the grate efficiency with respect to several parameters. In the first set, the interdependence of the void ratio and grate efficiency is investigated. In the second set of the experiments, the influence of the configuration on the hydraulic efficiency is studied. The final set of the experiments is performed to observe the grate efficiency of two successive grates. The result of each experiment is presented in detail.

Keywords: Hydraulic Efficiency, Transverse Grates, Void Ratio, Bypassed Flow, Intercepted Flow

ÖZ

YOLLARDAKİ ENLEMESİNE IZGARALARIN HİDROLİK VERİMLİLİKLERİNİN DENEYSEL OLARAK ARAŞTIRILMASI

Özbey, Cumhur

Yüksek Lisans, İnşaat Mühendisliği Bölümü

Tez Yöneticisi: Doç. Dr. Şahnaz Tiğrek

Aralık 2015, 84 Sayfa

Bu çalışmada, küçük yollarda kullanılabilecek enine ızgara sistemlerinin hidrolik verimlilikleri deneysel olarak araştırılmaktadır. Bu amaçla, ODTÜ Hidromekanik Laboratuvar'ında bulunan deney düzeneği kullanılmıştır. Yürütülen üç deney setinde, toplam debi ve ızgara verimliliği arasındaki ilişki farklı parametrelere göre incelenmiştir. İlk deney seti, boşluk oranı ve ızgara verimliliği arasındaki bağı araştırmaktadır. İkinci deney setinde, ızgara konfigürasyonunun hidrolik verimlilik üzerine olan etkisi çalışılmaktadır. Deneylerin son kısmı ise, ızgara verimliliği ve arka arkaya konulan ızgaraları gözlemlemek için gerçekleştirilmiştir. Her deney seti için bulunan sonuçlar, detaylı bir şekilde sunulmuştur.

Anahtar Kelimeler: Hidrolik Verimlilik, Enine Izgaralar, Boşluk Oranı, Geçen Akım, Tutulan Akım

To My Family & Friends

ACKNOWLEDGMENTS

TABLE OF CONTENTS

LIST OF TABLES

TABLES

LIST OF FIGURES

FIGURES

LIST OF SYMBOLS

b = Width of the Channel

d = Spacing between the Bars

k = Number of Spacing

k_s = Roughness Height of the Surface

l = Length of the Inlet along the Road

S = Longitudinal Slope of the Channel

S_r = Cross Slope of the Channel

Q_t = Total Flow

E = Efficiency of the Grate

Q_i = Intercepted Flow

Q_b = Bypassed Flow

E_s = Specific Energy

n = Manning Roughness Coefficient

y = Flow Depth

g = Gravitational Acceleration

Fr = Froude Number

Re = Reynolds Number

w = Grate width

x = Coordinate along flow direction

y = Coordinate along gravitational direction

y_1 = Upstream flow depth

y_2 = Downstream flow depth

μ = Fluid Viscosity

ρ = Density of the Water

v = Kinematic Viscosity of the Water

V = Flow Velocity

V_R = Void Ratio

CHAPTER 1

INTRODUCTION

1.1. General View

The analysis and the design of storm water drainage systems are an important topic as a whole including both hydraulic and hydrologic practices. Especially in urban areas, the correct design of surface drainage systems together with underground collection systems is essential to prevent flooding events. Furthermore, inadequate drainage of such storm water might generate an excessive amount of surface runoff or accumulation of water in urban streets and roads which may eventually cause hazardous situations for both vehicular and pedestrian traffic. This accumulation of water on the lanes of roads might trigger the rapid deterioration of the road and prevent pedestrian pass. Therefore, the main objective of drainage system design in roads is to reduce the potential risks by collecting the runoff and to transfer it to an underground system through inlet systems in an effective manner. Thus, safe travel conditions can be maintained and flooding of residential areas can be prevented.

Aim of the Study

The primary scope of this study is to provide a more general view and understanding of the storm water inlet systems when it is necessary to select an appropriate inlet for the drainage process of excess runoff. For this purpose, transverse grates which have various bar widths and orientations have been tested under different approaching flow conditions in the Hydromechanics Laboratory of Middle East Technical University in order to estimate their efficiencies. The

experimental study is conducted by utilizing an experimental setup including a platform which acts as a small road where a number of grated inlets are placed and tested.

1.2. Outline of the Thesis

In this study, transverse grate inlets having different bar widths and patterns are examined and the interception of flow by these varying systems is observed aiming to compare each other in terms of efficiencies and geometric conditions. After introducing the problem and explaining the general scope of the study in the first chapter, in Chapter 2, methodological and theoretical concepts and several past studies related to this subject are presented. In Chapter 3 the experimental setup and the grates in detail are presented. In Chapter 4, results of the laboratory experiments are reported in tables and graphics. Additionally, hydraulic efficiencies of the grates are analyzed with respect to different discharges, grate geometries and configurations. Finally, in Chapter 5, findings of the conducted set of experiments and suggestions for future studies are listed as a conclusion part.

CHAPTER 2

THEORETICAL CONCERNS

New developments or improvements of existing drainage systems can be necessary due to the increase in urbanization since human beings do not want to stand for the inconvenience and to be affected by loss of life. Therefore, storm water management systems have been taken into consideration in order to provide safety and convenience. Furthermore, removing the runoff as rapidly as possible by means of an appropriate drainage system is expected to be fulfilled, no matter how intense and how long the duration of the rainfall is (Jones, 2006). Storm water runoff is generally transported by means of grate and curb inlets that are positioned in street gutters and sump locations (Comport and Thornton, 2012).

Eliminating storm water in highways in a cost-effective and rapid manner can be regarded as a fundamental consideration in the drainage systems (Huebner et al., 1986). There are two main objectives of the usage of residential storm water runoff systems: preventing loss of life and property as well as providing adequate level of convenient access to property throughout or after the rainfall. Thus, convenience and safety at the subdivision and at the drainage basin level must be taken into consideration for a storm water system design (Jones, 2006). Moreover, the flow in the gutter, the type and the location of the inlet affect the hydraulic capacity of an inlet structure. Therefore, inlets on curbed gutters should be placed according to their capacities, flow in gutter and the tolerable extent decided by considering the traffic safety (Pazwash and Boswell, 2003).

With the purpose of decreasing the danger and the destruction caused by the intense storm water in urban areas, the accurate design of surface drainage systems should be achieved (Russo et al., 2013). The ideal inlet design requires the most efficient combination of the inlet type, size and location depending on the gutter spread with the highest width (Nicklow and Hellman, 2000).

2.1. Literature Review

Since the interception capacity of inlet systems alters depending on the highway variations and inlet geometry, laboratory research that examine the performances of inlets (Izzard 1950; Bauer and Woo 1964; Uyumaz 1992; Hammonds and Holley 1995; Fang, Jiang and Alam, 2010; Guo, MacKenzie and Mommandi, 2009) maintain its importance. As an example, Guo et al., (2009) revealed that the interception capacities of various sump inlet types such as 3-5 ft curb opening inlets, bar and vane grates exhibit remarkable differences in the laboratory experiments. These tests are conducted by considering HEC 22 design procedure which includes a 1/3-scale laboratory model with a 3.5 m wide flume to form street flow over a sump inlet. As a result, they developed new formula and procedures with the coefficients adjusted by the data gathered through laboratory tests.

In another study, Fang et al., (2010) upgraded models to simulate unsteady, free-surface, shallow flow through curb-opening inlets by utilizing a three-dimensional computational fluid dynamics (CFD) software, FLOW-3D.

Comport and Thornton (2012) examined a curb inlet and two combination inlets in accordance with the different road conditions by means of designing a one-third Froude-scale model of a two-lane road section and they developed equations for practical applications.

Sipahi (2006) designed and constructed an experimental setup in the Hydromechanics Laboratory of Middle East Technical University to examine the differences in the interception capacities of grated inlets with respect to various flow

conditions. A rectangular channel was utilized to study the interception of flow by means of preliminary experiments conducted on the tilting flume. Therefore, the functioning of the newly designed setup and the calculation of the grate efficiencies were achieved according to the longitudinal slope and the Froude number. The results of the study indicated that this designed setup could be utilized in order to perform experiments for obtaining a common expression for grate efficiency.

Sezenöz (2014) conducted a numerical study to analyze recently planned grated inlet system for small roads. For this reason, Flow 3D software was used to model the physical conditions of the setup including a rectangular channel of 0.9 meters width and continuous transverse grate system which was located on the basis of the setup constructed in the Hydromechanics Laboratory of METU. The results obtained in this study were compared with the previous ones that had been based on the experimental data collection. In the numerical model, the system's channel capacity was increased to be able to observe the performance of the system in respect of higher amounts of flow rates. The efficiencies of continuous transverse grate were computed for different amounts of flow rates and consequently, their interactions with total flow rates and Froude numbers were displayed.

Hydraulic efficiency of continuous transverse grates for paved areas was investigated by Gomez and Russo (2005, 2009 and 2011) in the laboratory of the University of Catalonia Hydraulic Department. Although it is a laboratory study, they kept the dimensions of the grates as it is, thus the grates of full scales on a 1.5 m wide and 5.5 m long rectangular testing area was used for the tests. The flow was discharged by pump systems including a tank located about 15 m above the platform and an electromagnetic flow meter was utilized in the calculation of the discharge. A V-notch triangular weir was used for the conveyed discharge by the inlet and the calculation of the flow was handled by a limn meter with an accuracy of 0.1 mm. Unit discharge was used for the computation of the efficiency of the inlet system.

Şahin (2006) conducted a study to determine the most efficient drainage inlet type by using the experiments that were held by FHWA (Federal Highway Administration). These experiments included six different grate types with various bar configurations and longitudinal slopes. Two dimensionless parameters were obtained as a result of these experiments for all of the grate types that were tested. Thus, it was stated in the study that the hydraulic performance of the grates that have bars parallel to the flow direction was better than the transverse bar grates.

Mustaffa (2003) investigated the hydraulics of street inlets with respect to various coefficients by using Reynolds number and Froude number. Different configurations of grate inlets that were located in reservoirs and channels were used and also an orifice-oriented inlet was utilized for single orifice, multiple orifices and orifices with a certain amount of roughness on the surrounding bed. The results indicated the differences in the discharge coefficients which were appropriate to the calculation of the actual flows entering the inlet for various flow conditions.

Jiang (2007) investigated the performance of inlets basically for lower values of longitudinal and cross slopes. Numerical modeling simulation, FLOW-3D software, was utilized to examine the efficiency of the drainage inlets under different geometric settings of various longitudinal grades and cross slopes. The results pointed out that for a certain type of curb opening inlet, there is a linear relationship between the cross slope of the channel and the intercepted flow at varying longitudinal slopes. As a result, corresponding linear equations were developed by considering the results of the simulation model.

To sum up, most of the research in the literature concerning the efficiency of grate inlets for different parameters has been done by using simulation models and software programs. Although there are laboratory experiments for observing the efficiency of inlets with respect to the flow rate as well as the longitudinal and cross slope and certain bar configurations, it is still essential to conduct further experimental observations due to variety of grate geometry and configurations.

Tiğrek and Sipahi (2011) suggest a grate to small roads based on the experimental work of Sipahi (2006). They suggested that small roads which do not have underground collection systems can act as conveyance channels and water can be transferred to the underground channel of big streets by collecting storm water runoff at the end of the road. The range of the discharge was small while comparing available commercial grates. Therefore, in the present study, it is aimed to extend the laboratory investigation of Sipahi (2006) in order to investigate some other parameters such as void ratio, configuration and multiple grates.

2.2. Inlet Structures

The main target of highway drainage design is to convey the storm water runoff into subsurface storm sewers by means of inlets that have to provide maximum safety for vehicles, bicycles and pedestrians, as well as having minimum material and construction cost (Nicklow and Hellman, 2000). Inlet constructions are generally made up of the materials such as cast-in-place concrete or pre-cast concrete. Inlets are usually placed in gutter sections, paved medians, roadsides and median ditches. The structure of an inlet is composed of a box structure which includes an opening in order to capture storm water (Sipahi, 2006). Parameters that affect the interception capacity of the inlets are the types of inlet, the number of inlets to be constructed, the selected size and the specified location of each inlet (Nicklow and Hellman, 2000).

2.2.1. Inlet Types

The drainage system constructions that are used for accumulating the surface water by means of grate or curb and for transmitting it into the sewers are called **inlets**. As displayed in Figure 2.1, inlets in the highway surfaces are classified as in the following categories (HEC 22, 1991):

- *Grate Inlets* are the ones that contain opening in the gutter which is enfolded by one or more grates.

- *Slotted Inlets* consist of pipe cut along the longitudinal axis with bars to maintain slot opening.
- *Curb Opening Inlets* are perpendicular openings in the curb covered by a top slab.
- *Combination Inlets* are the ones that contain adjacent construction of a curb opening inlet and a grate inlet. However, the curb opening might be placed in the upstream part of the grate.

Grate Inlet
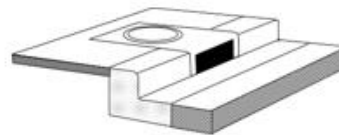
Curb Opening Inlet

Slotted Inlet
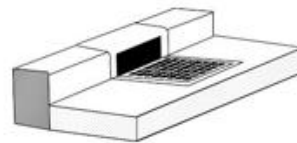
Combination Inlet

Figure 2.1 Inlet types (see HEC 22, 1991)

The performance of an inlet purely relies on its bar geometry and the cross slope, longitudinal slope, total gutter flow, depth of flow and pavement roughness. The depth of the storm water next to the curb has the major influence on the interception capacity of gutter inlets and curb opening inlets. Moreover, at low velocities of the runoff, more amount of water is conveyed compared to the runoff at higher velocities.

If the performance of an inlet is not sufficient, bypassing water might result with flooding on the highways which may eventually lead to a road destruction or a traffic disruption (Pazwash and Boswell, 2003). Furthermore, unless the holes of the inlets are large enough, they are covered by leaves and dust hindering the storm water from running into the sewers (Fujita, 2002).

The most effective type of gutter inlet is parallel bar grate. However, its efficiency is decreased when crossbars are added in order to provide bicycle safety. For a design concerning the bicycle traffic, the curved vane grate and the tilt bar grate are suggested due to their features like hydraulic capacity and safety conditions for bicycles (HEC 22, 1991). Besides, more debris can be handled by these grates provided that the vanes of the grate are placed in the proper direction. However, for the highways with debris problem, the debris handling efficiency levels of grate inlets should be considered by conducting relevant laboratory experiments.

2.3. Interception Capacity of an Inlet

Interception capacity of an inlet can be defined as the ratio of the intercepted flow taken by the inlet to the total flow which can be described as the sum of the intercepted flow and the bypassed flow passing through the grates. Thus, efficiency (E) can be calculated by the following equation:

$$E = Q_i / Q_t \tag{2.1}$$

where, Q_t is the total approaching flow, which includes the intercepted flow rate (Q_i) and bypassed flow rate (Q_b) and it is calculated as follows:

$$Q_t = Q_i + Q_b \tag{2.2}$$

The hydraulic performance and the efficiency of an inlet vary depending on the following parameters:

- ➤ longitudinal slope of the road
- ➤ cross slope
- ➤ total gutter flow
- ➤ pavement roughness
- ➤ geometry of the paved area
- ➤ clogging factors
- ➤ bar geometry

In general, efficiency of inlets decreases and the interception capacity of inlets increases when the flow rate increases. This is mainly due to the fact that the interception capacity of a grate inlet and its efficiency depend on the amount of runoff and its velocity as mentioned previously in above sections. In addition to these hydraulic parameters, geometric parameters such as the size, grate configuration, grate type, distance between the parallel bars and arranging style of these bars should be taken into consideration for the calculation of the efficiency and interception capacity of grate inlet systems. Therefore, in this study interception capacity and the corresponding efficiencies of grated inlets are examined in terms of flow rate, grate configuration and void ratio. Accordingly, various significant results have been obtained throughout the laboratory experiments of this study which can be utilized to point out the suggestions to improve the efficiency of inlet systems.

2.4. Flow through Grated Inlets

The passage of water through a grate inlet could be regarded as one of the most remarkable examples of **spatially varied flow** in which the discharge decreases in the flow direction along the channel even though the flow is under steady-state condition. Since certain amount of flow is captured by the openings of the inlet, flow

rate will be undoubtedly decreased at the exit section of the grate. This type of flow can be modeled as a channel having a frame which is formed by bars parallel to the flow direction at the bottom part, representing a grated inlet system. Figure 2.2 illustrates the flow passing over a grate inlet where x-axis denotes the direction of flow whereas y-axis stands for the vertical direction related to the depth of flow.
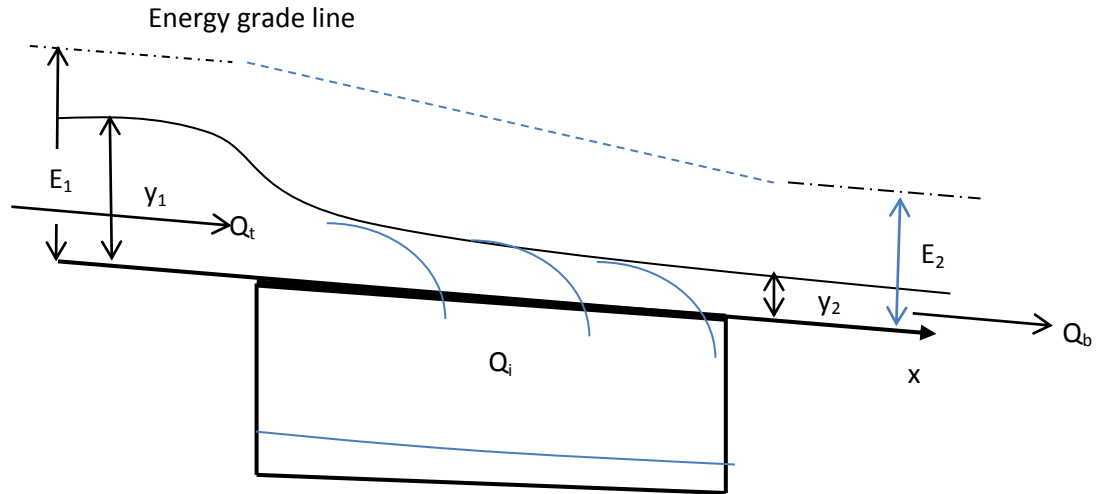
Figure 2.2 Passage of water through grate inlet (Sipahi, 2006)

In general, by utilizing the values of flow depth, y, discharge, Q, and width of the channel, b, the specific energy (E_s) can be expressed at any arbitrary section as in the following equation;

$$E_s = y + \frac{Q^2}{2gy^2b^2} \tag{2.3}$$

Then, from this equation, discharge is found as;

$$Q = by\sqrt{2g(E_s - y)} \tag{2.4}$$

The flow passing through a grated inlet while running the experimental setup is also shown in Figure 2.3.

Figure 2.3 Flow passing through a grate inlet

2.5. Dimensional Analysis

The efficiency of a grated inlet system is affected by many parameters and hence, by changing certain conditions of the testing setup, different variations could be obtained in accordance with the hydraulic performances of the grates. Therefore, a dimensional analysis is carried out so as to perceive the variables that have some obvious influence on the hydraulic performances of the grate inlet systems. So, corresponding parameters are presented as follows:

In Figure 2.2, x and y denote the axis along the flow direction and the gravitational direction, respectively. E_s [L] is the specific energy at the beginning of the grated inlet. y_1 [L] and y_2 [L] are the flow depths at the upstream and downstream of the inlet. The length of the inlet along the road is l [L]. The intercepted flow, Q_i [L^3/T] is the difference between the total channel flow, Q_t [L^3/T] and the bypassed flow, Q_b [L^3/T] as expressed in the following equation;

$$Q_i = Q_t - Q_b \tag{2.3}$$

The intercepted flow can be written as a function of twelve variables as given below;

$$Q_i = f_1 (Q_t, y_1, b, k_s, g, \rho, v, w, l, d, k, S, S_r) \tag{2.4}$$

in which b [L] is width of the channel; w [L] is width of the grate, k_s [L] is roughness height of the surface; g [L/T^2] is the gravitational acceleration; v [L^2/T] is the kinematic viscosity of the water; ρ [M/L^3] is the density of the water, d [L] *is* the spacing between the bars, k is the number of spacing, S and S_r are the longitudinal and cross slopes, respectively. If ρ, Q_t and y_1 are selected as repeated variables:

$$\pi_o = f_2 (\pi_1, \pi_2, \pi_3, \pi_4, \pi_5, \pi_6, \pi_7, \pi_8, \pi_9, \pi_{10}) \tag{2.5}$$

$$\frac{Qi}{Qt} = f_3 (\frac{y_1^5 g}{Q_t^2}, \frac{y_1 v}{Q_t}, \frac{b}{y_1}, \frac{w}{y_1}, \frac{k_s}{y_1}, \frac{l}{y_1}, \frac{d}{y_1}, S, S_r, k) \tag{2.6}$$

If the first π-term multiplied by third one, reciprocal of the result will give square of the Froude number, Fr is expressed below,

$$\pi_{11} = \frac{1}{\pi_1} * (\frac{1}{\pi_3})^2 = \frac{Q_t^2}{g y_1^3 b^2} = Fr^2 \tag{2.7}$$

and the reciprocal of the multiplication of second and third π-terms will give the Reynolds number, Re, as explained below,

$$\pi_{12} = \frac{1}{\pi_2} * (\frac{1}{\pi_3}) = \frac{Q_t y_1}{b y_1 v} = Re \tag{2.8}$$

Thus, the Froude number, Fr will be summarized as a function of upstream water depth (uniform flow depth), y_1 and the total discharge, Q_t as follows;

$$Fr = \frac{Q_t}{\sqrt{9.81b^2 y_1^3}} \tag{2.9}$$

In addition, $\pi_{13} = (\pi_7 * \pi_{10}/\pi_4) = kd/b$ will be described and called as the void ratio, V_R.

Further if the efficiency, E is described as the ratio of the intercepted flow to the total flow (FHA 2001), then it is expressed as,

$$E = \frac{Q_i}{Q_t} \tag{2.10}$$

Thus, $\pi_o = Q_i/Q_t$ will be equal to the efficiency. In this study, the width of the channel, which is 0.90 meters, is a constant parameter in the experimental setup and the surface of the main channel is all made up of fiber glass which enables to ignore the effect of surface roughness. In addition to these, the longitudinal slope of the channel is kept constant and the cross slope is zero. If one considers the flow to be a fully turbulent flow, the following dimensionless variables are the parameters of the study:

$$E = f_3 (F_r, V_R) \tag{2.11}$$

Finally, since the total flow is a function of both intercepted and bypassed flows, it could be dropped in the equation as well. Thus, since the effect of Reynolds number is negligible, it can be concluded that the grate efficiency is mainly affected by the total approaching discharge and the flow depth as well as the dimensionless parameter, Froude number which is discussed in Chapter 4.

CHAPTER 3

EXPERIMENTAL SETUP

A testing setup was constructed in the Hydromechanics Laboratory of METU in 2006 by Sipahi in order to observe the flow passing through a grate. This current study is basically conducted for determining the interdependence of grate efficiency with respect to certain parameters. Hydraulic performance, interception capacity and efficiency of this already-constructed inlet system are investigated by testing various types of grates as well as changing the grate orientation.

In this study, hydraulic performance, interception capacity and efficiency are used interchangeably; in other words, the hydraulic performance and interception capacity refer to the efficiency of the inlet system. Various details and dimensions related to the main channel of the setup, discharge channels, collective pools and grated inlets are presented in the following sections. Figure 3.1 shows a general view of the experimental setup.

Figure 3.1 General view of the setup

3.1. Main Channel

The experimental system is basically formed over a main channel having a length of 12 meters which represents a small road section in order to observe the performances of different inlet structures. The channel enables to utilize the following longitudinal slope values: S=0, S=1/300, S=1/100, S=1/50 and S=1/25. However, all the experiments have been conducted for the longitudinal slope of S=1/300 in this current study in order to examine subcritical flow conditions in more detail. The higher slopes result in supercritical flow. Further, S=0 slope was examined in detail in the previous study (Sipahi, 2006) and the flow condition for that slope was subcritical. In addition to the longitudinal slope, cross slope of the main channel is another factor which inevitably affects the interception capacity of an inlet system. Nevertheless, zero percent cross slope is utilized in this study due to the limitations of the laboratory conditions.

The main channel of the system was made up entirely of fiber glass even though it was initially constructed by steel and it allows maximum 10 cm of water depth as a runoff that could be formed over the surface of the channel. Corresponding dimensions related to the width and height of the main channel sections are presented in Figure 3.2 below.
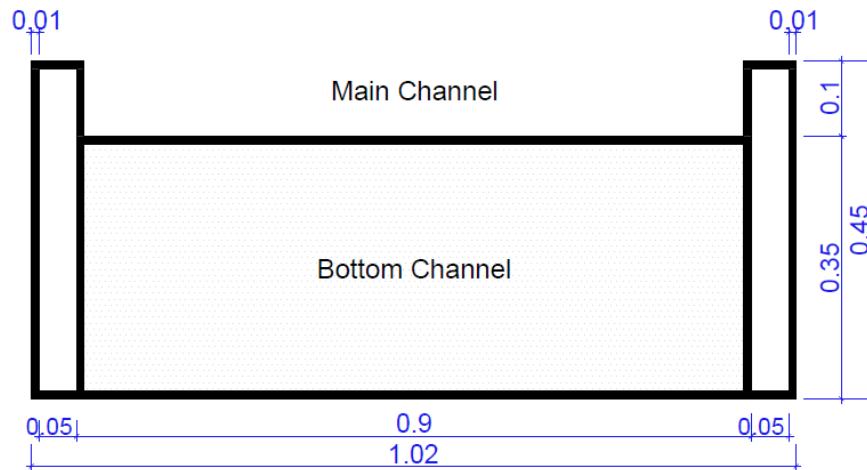
Figure 3.2 Main Channel (All dimensions are in meters)

When regarded as a whole, the main channel is constructed of 1.0 meter blocks to ensure a smooth surface for the passage of water coming from the upstream. Moreover, with the purpose of preventing the leakage between two consecutive blocks, a special cement is pasted at the connections.

3.2. Discharge Channels

As a total, the experimental setup provides to conduct experiments for three grates. Even though only a single grate was tested in Sipahi's study in 2006, this current study enables to test the hydraulic performances of three grates in which they were all executed either one by one or by a combination of them.

Each grate has its own discharge channel which is located below the surface of the main channel. Due to the fact that there are three discharge channels throughout the width of the main channel whose length is 0.90 meters, each discharge channel can have a maximum allowable width of 0.30 meters. The corresponding dimensions of each discharge channel are illustrated in Figure 3.3.
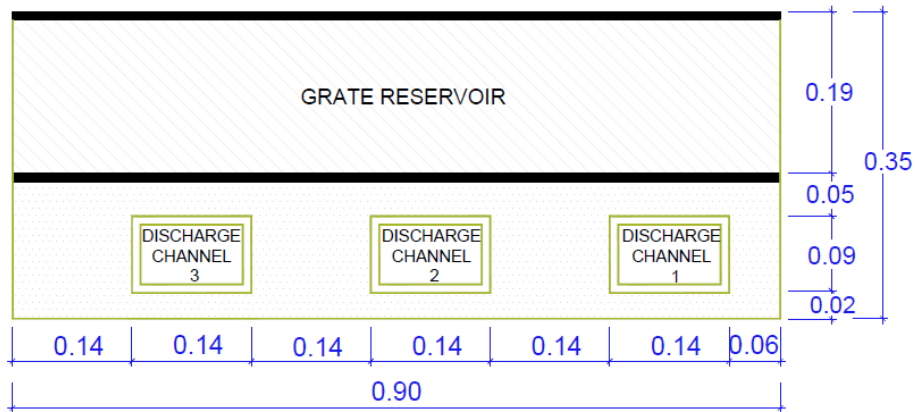
Figure 3.3 Cross-Section of Discharge Channels (All dimensions are in meters)

Figure 3.4 illustrates a three dimensional view of the discharge channels during their operation.
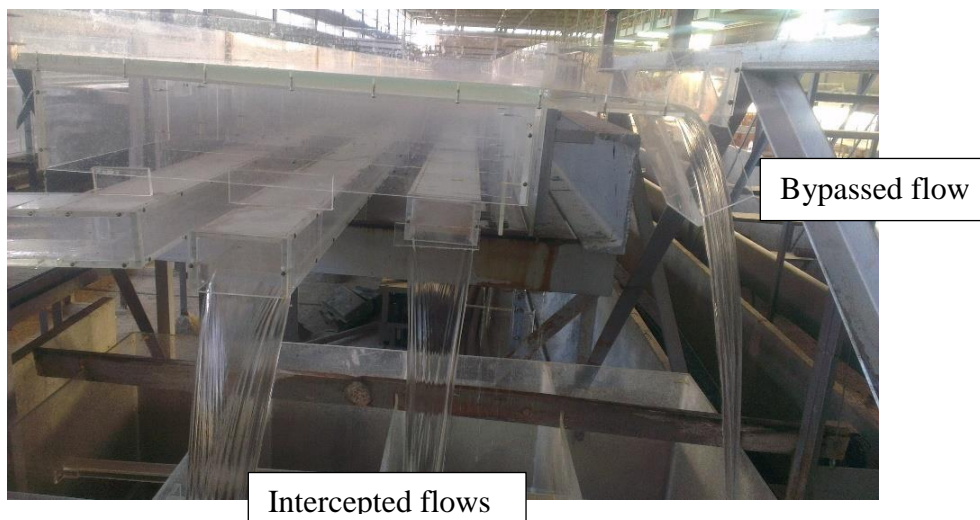
Figure 3.4 Discharge channels during operation

3.3. Collecting Pools

In the experimental setup, there are four pools at the end section of the main channel which serve as a collective system. The pools are utilized to maintain the accumulation of water coming from the discharge channels either one by one or simultaneously, as well as to gather the bypassed flow which is not intercepted through the grates.

Pools are made up of fiber glass, which is the same material with the main channel and all four pools have the thickness of 0.15 meters and also the other dimensions are identical for each pool as shown in Figure 3.5.
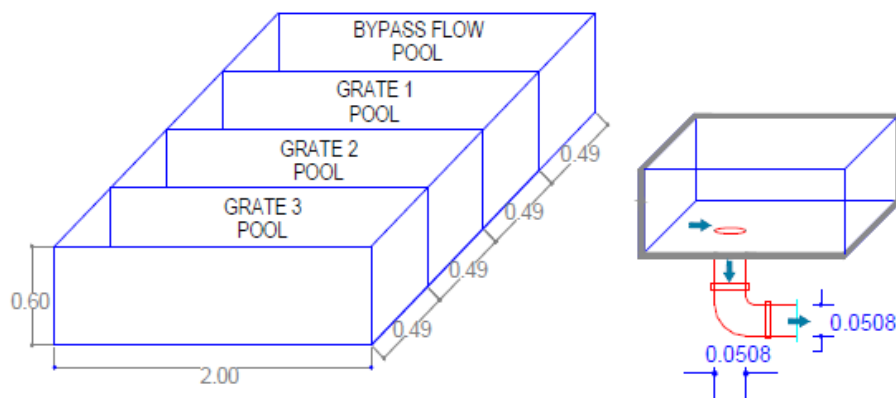
Figure 3.5 Details of the Collective Pools (Sipahi, 2006) (All dimensions are in meters)

During the collection of water in the pools, as the depth of water increases, inevitably the pressure exerted to the side walls of the pools increases as well. Therefore, in order to cope with this pressure increase without causing any cracks or a total failure of the collective system, fiber glass rods are placed laterally inside the pools aiming to strengthen the structure as a whole.

The values of the intercepted and bypassed flow rates are computed by considering the amount of water rise (in cm) during a certain period of time (in sec). For this purpose, each pool has its own piezometric tube having a scaled paper on it for the observation of the volumetric water level rising inside the pool. However, the fact that pools have a finite volume of 0.59 m^3 each causes an unavoidable restriction for performing the experiments for relatively higher values of flow rates.

During the process of emptying out the pools, each pool has a discharge pipe that is just placed beneath it as shown in Figure 3.5. Additionally, in order to evacuate the accumulated water rapidly, each pipe has a valve that can be opened or closed whenever wanted while conducting the experiments and especially throughout the data collection for the observation of water rising in the pools.

A general perspective of the collective system while operating the intercepted and bypassed pools is shown in Figure 3.6.

Figure 3.6 Collective Pools

3.4. Experimental Sets

In the experimental setup, the first grate is located at the 9th meter of the main channel which can be regarded as a section that is relatively towards the end of the channel. Thus, developed flow conditions can be maintained as much as possible.

As shown in the general top view of the setup in Figure 3.7, there could be three possible locations (sections 1, 2 and 3) for the grated inlets to be placed and they could be utilized either one by one or by using a combination system throughout the experiments.
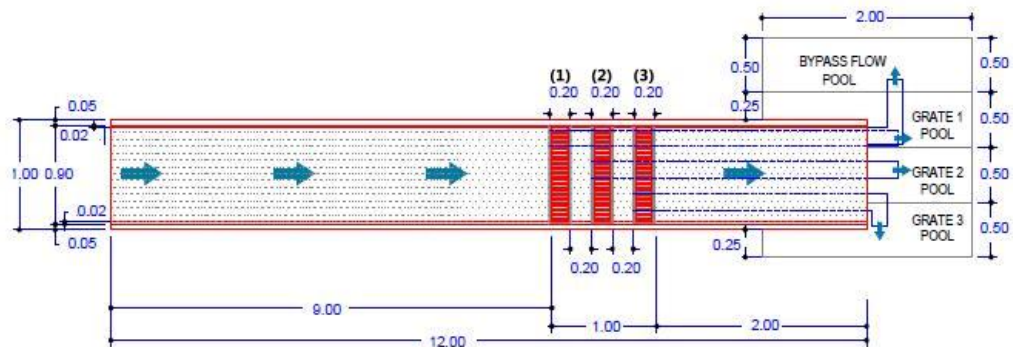
Figure 3.7 Top view of the experimental system (Sipahi, 2006) (All dimensions are in meters)

The water coming from the upper part of the channel is intercepted by these grates and conveyed to the collective system pools by means of discharge channels that are located just underneath of each grate section. The remaining bypassed water which is not captured by the grated inlet is carried till the end of the channel where it finally falls into the pool which is responsible for collecting the bypassed flow. Provided that two or more grates are tested simultaneously on the main channel, the water which is not intercepted by the first grate is captured by the subsequent grate or grates, respectively.

3.4.1. Experimental Set A: Void Ratio

As stated in the previous chapters, the main objective of this study is to investigate the hydraulic performance of the grated inlet systems by examining the relationship between the total flow and the grate efficiency with respect to certain parameters.

3.4.1.1. Grate Details

For the first part of the experimental procedure, six different continuous transverse grates are utilized, each having different spacing between the grate bars resulting in different void ratios. Grates are placed one by one at the first grate section and they are observed for their performances in accordance with the total approaching flow. Below, corresponding bar and spacing details of these six continuous grates are presented from Figure 3.8 to Figure 3.13.
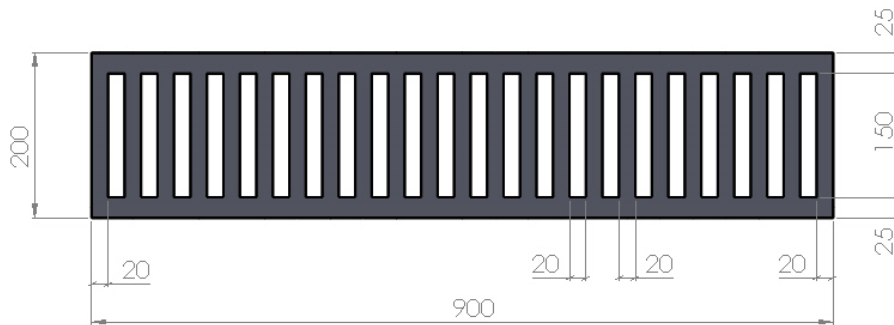
Figure 3.8 Grate bar of 2 cm with 2 cm spacing (All dimensions are in mm)
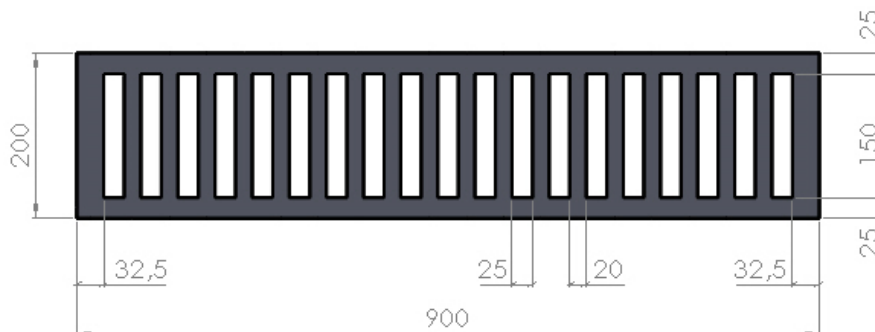
Figure 3.9 Grate bar of 2 cm with 2.5 cm spacing (All dimensions are in mm)
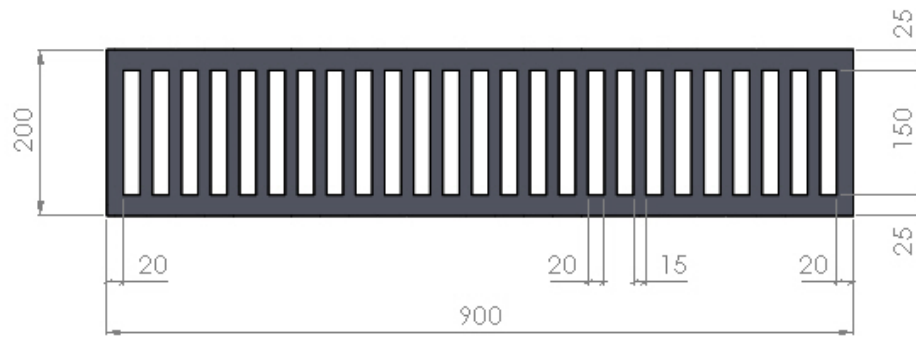
Figure 3.10 Grate bar of 1.5 cm with 2 cm spacing (All dimensions are in mm)
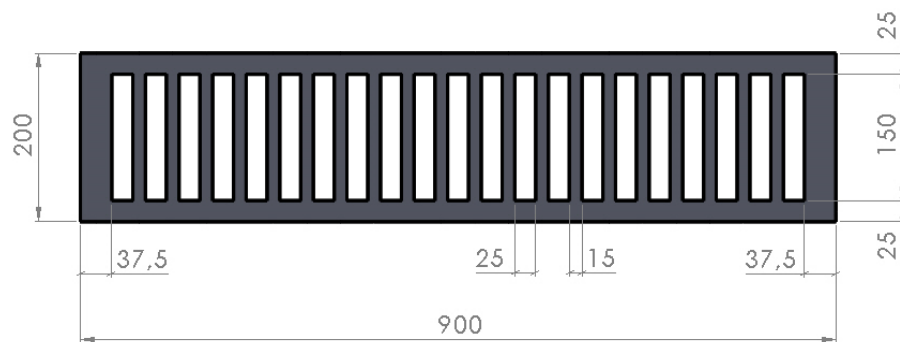
Figure 3.11 Grate bar of 1.5 cm with 2.5 cm spacing (All dimensions are in mm)
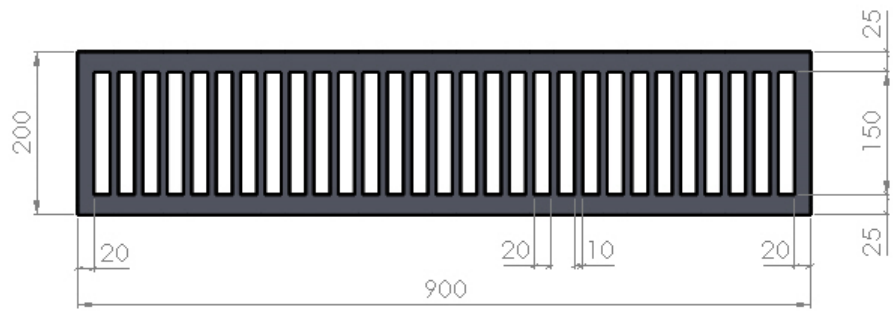
Figure 3.12 Grate bar of 1 cm with 2 cm spacing (All dimensions are in mm)
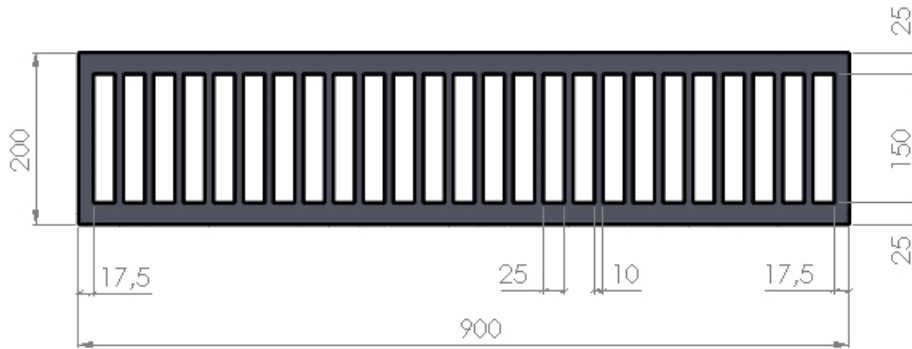
Figure 3.13 Grate bar of 1 cm with 2.5 cm spacing (All dimensions are in mm)

3.4.2. Experimental Set B: Configuration

In the second part of the experimentation, a specific case is tested by using two different configurations of the grated inlets and the corresponding hydraulic efficiencies of the grates are compared with respect to the total discharge. For this reason, two types of grates are placed one by one only at section (1), the first type having grated bars only on the left part according to flow direction and the second type having grated bars symmetrically on both sides with a full middle part. Corresponding bar details and dimensions of the two grates are shown in Figure 3.14 and in Figure 3.15. In addition to these, Figure 3.16 displays a top view of the grate having bars on both sides.
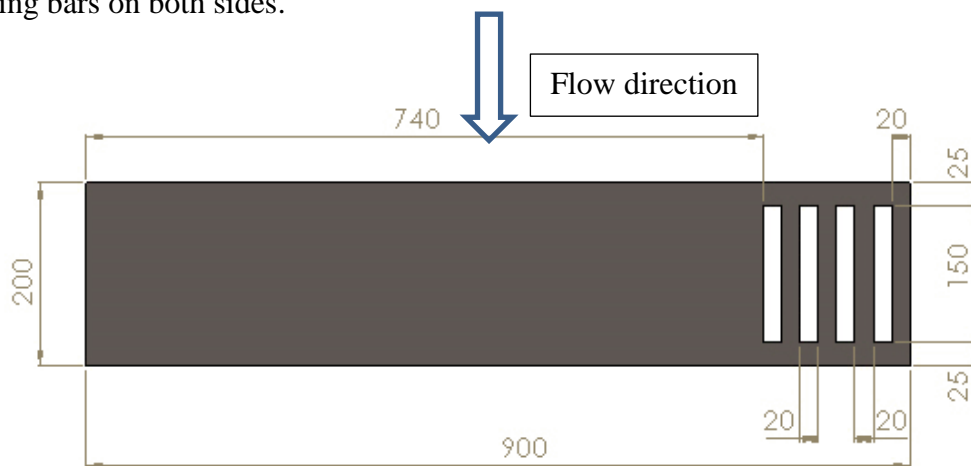
Figure 3.14 Grated bars only on the left part (All dimensions are in mm)

Figure 3.15 Grated bars on both sides with full middle part (All dimensions are in mm)

Figure 3.16 Grated bars symmetrically on both sides

3.4.3. Experimental Set C: Distance between Grates

In the final set of the conducted laboratory experiments, another specific case is investigated by utilizing two grates having different distances between them. For the first case, the inlet that has grated bars only on the left part is placed at the first section and the inlet having grated bars only on the right part is located at the second

section. Hence, corresponding hydraulic performances are examined by running the system simultaneously. Likewise, for the second case, grates are placed at the first and third sections respectively and again the efficiencies are investigated by testing the grates at the same time. Therefore, the influence of the interval between two successive grates on the hydraulic efficiency is studied. Below, spacing and bar dimensions are presented in Figure 3.17 and in Figure 3.18.
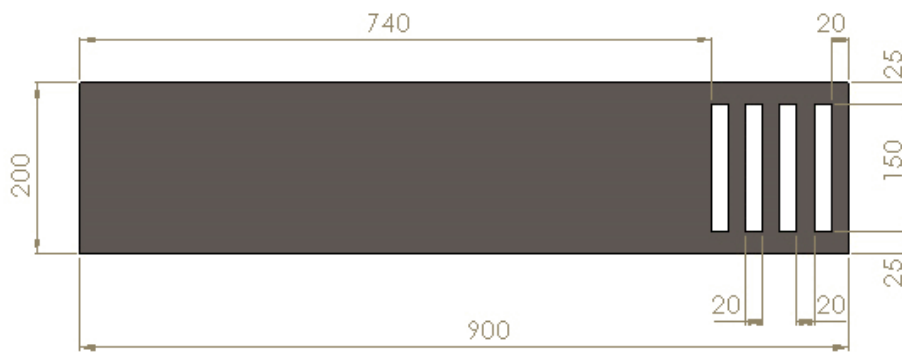
Figure 3.17 Grated bars only on the left part (All dimensions are in mm)
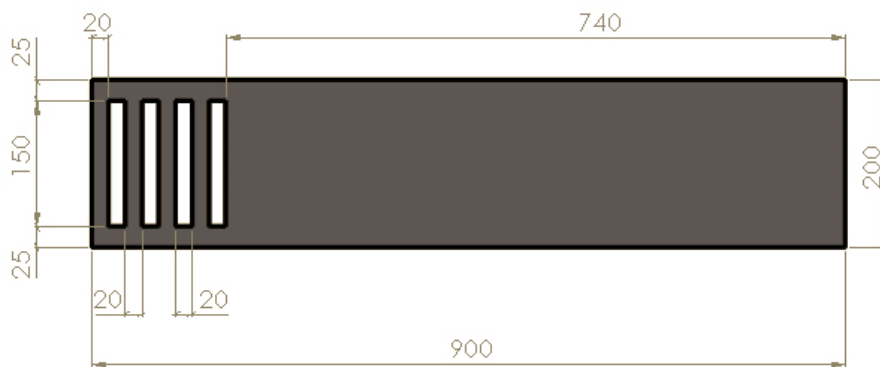
Figure 3.18 Grated bars only on the right part (All dimensions are in mm)

A general display of the system including two grates that are operating concurrently is illustrated in Figure 3.19.

Figure 3.19 General view of the grates at section (1) and (2).

CHAPTER 4

RESULTS AND ANALYSIS

In this chapter, the tabular and graphical results of various experiments that have been conducted in the Hydromechanics Laboratory of METU will be presented. First of all, results will be given and analyzed with respect to the **void ratio** considering the varying total approaching flow. In the second part, **grate orientation** will be taken into consideration and the corresponding results will be handled.

4.1. Total Flow versus Efficiency: Void Ratio

In this part of the study, for the void ratio aspect, six different types of **continuous transverse grates** have been examined by means of laboratory experiments, each having a certain distance between the parallel bars resulting in specific void ratios. The widths of the grates are different as well. Then, for each six case, the dependence for the total discharges coming from the upstream and the corresponding grate efficiencies are presented and are analyzed by tables and graphics.

4.1.1. Distance and Arrangement of Parallel Bars

Six types of continuous grates each having a different distance between the parallel bars are investigated in order to examine their interception capacities and corresponding hydraulic efficiencies. All of the laboratory data for each case are presented in Appendix A.

> ➤ **Case A1:** V_R = 37.56 % (2 cm gap – 2 cm full)

The obtained data for the first case including the grated inlet with bar distance of 2 cm gap – 2 cm full (V_R = 37.56 %) are displayed in Table 4.1 and in Figure 4.1.

Table 4.1 Total discharge and efficiency values for V_R = 37.56 %

Q_t (10^{-4} m³/s)	Efficiency (%)
18.307	92.290
18.806	91.790
36.395	91.976
37.568	90.256
45.141	90.401
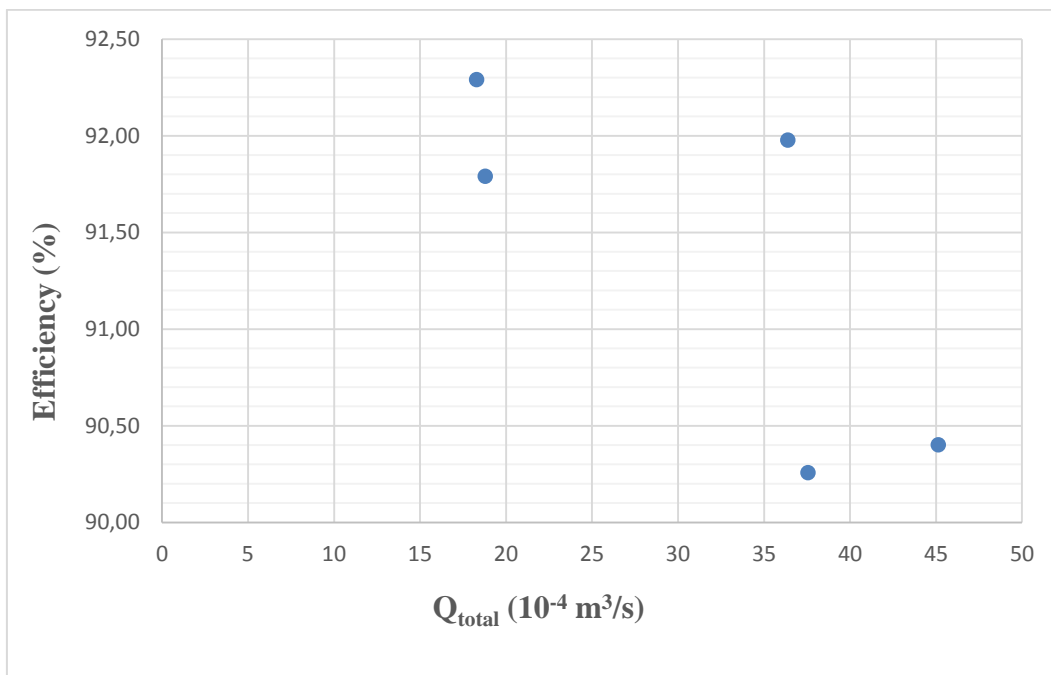
Figure 4.1 Total discharge versus efficiency for V_R = 37.56 %

In 2006, Sipahi conducted experiments at the same experimental setup for different values of the longitudinal slope of the main channel in order to observe the relationship between the total approaching discharge and efficiency of the grated inlet. In Figure 4.2, the interdependence between the total flow rate and efficiency values of this study is compared with the study executed by Sipahi in which the identical 2 cm gap – 2cm full grated inlet was tested for the same longitudinal slope of S=1/300. The figure shows that although the trend of two set of experiments can be accepted to be similar, there are big percentage differences between the values. It may be due to measurement techniques of discharge. The pool dimensions might be too big for discharges since it depends on the observation in water depth by naked eye. Furthermore, the elapsed time between two experiments is too long such that the fiber glass, the main construction material of the channel and pools might be deformed.
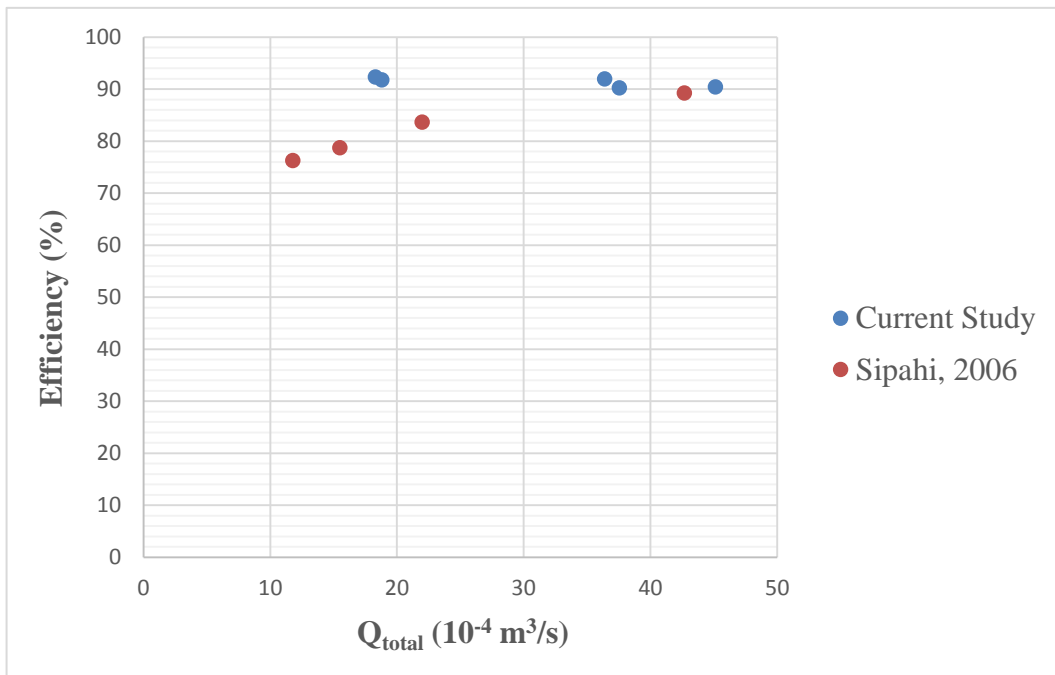
Figure 4.2 Comparison of the efficiency with Sipahi, 2006 for S=1/300

> **Case A2:** $V_R = 40.55\ \%$ (2.5 cm gap – 2 cm full)

The data concerning the second case that include the grated inlet with bar distance of 2.5 cm gap – 2 cm full ($V_R = 40.55\ \%$) are shown in Table 4.2 and in Figure 4.3.

Table 4.2 Total discharge and efficiency values for $V_R = 40.55\ \%$

$Q_t\ (10^{-4}\ m^3/s)$	Efficiency (%)
15.525	89.079
22.525	89.977
36.032	90.000
52.058	91.435
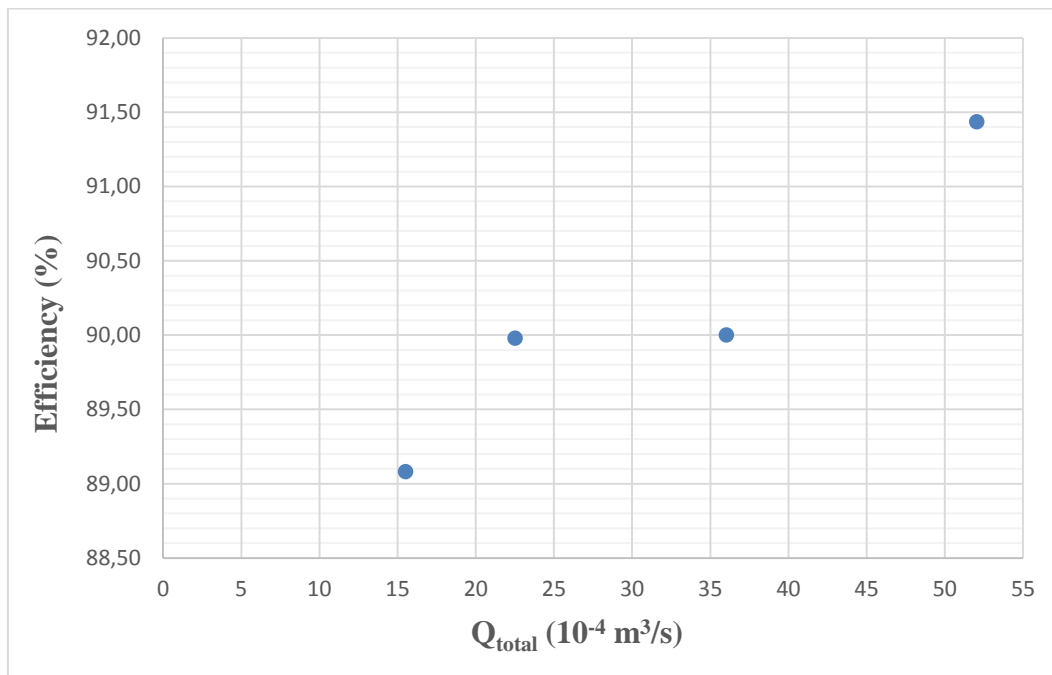
Figure 4.3 Total discharge versus efficiency for $V_R = 40.55\ \%$

> **Case A3:** $V_R = 42.6 \%$ (2 cm gap – 1.5 cm full)

The data for the third case that are collected for the grated inlet with bar distance of 2 cm gap – 1.5 cm full ($V_R = 42.6 \%$) are listed in Table 4.3 and in Figure 4.4.

Table 4.3 Total discharge and efficiency values for $V_R = 42.6 \%$

$Q_t (10^{-4} \, m^3/s)$	Efficiency (%)
35.793	92.789
40.342	93.166
44.544	93.505
49.838	93.409
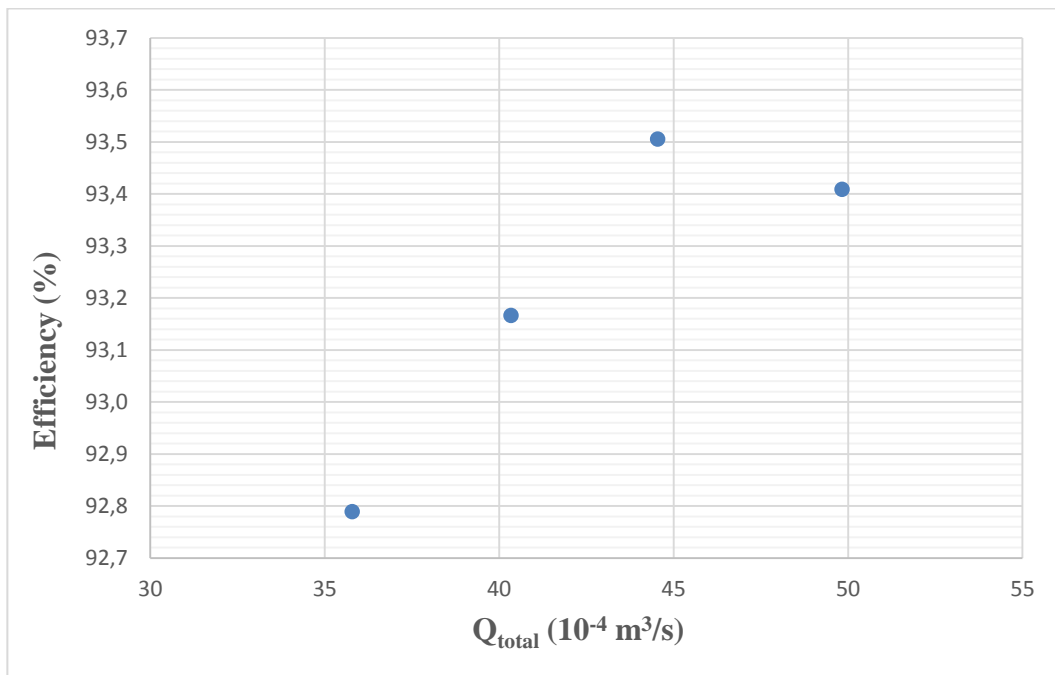
Figure 4.4 Total discharge versus efficiency for $V_R = 42.6 \%$

➢ **Case A4:** $V_R = 44.8$ % (2.5 cm gap – 1.5 cm full)

The gathered data for Case A4 concerning the grated inlet with bar distance of 2.5 cm gap – 1.5 cm full ($V_R = 44.8$ %) are shown in Table 4.4 and in Figure 4.5.

Table 4.4 Total discharge and efficiency values for $V_R = 44.8$ %

Q_t (10^{-4} m^3/s)	Efficiency (%)
15.484	93.217
21.578	93.597
34.868	93.614
47.591	93.805
51.575	94.120
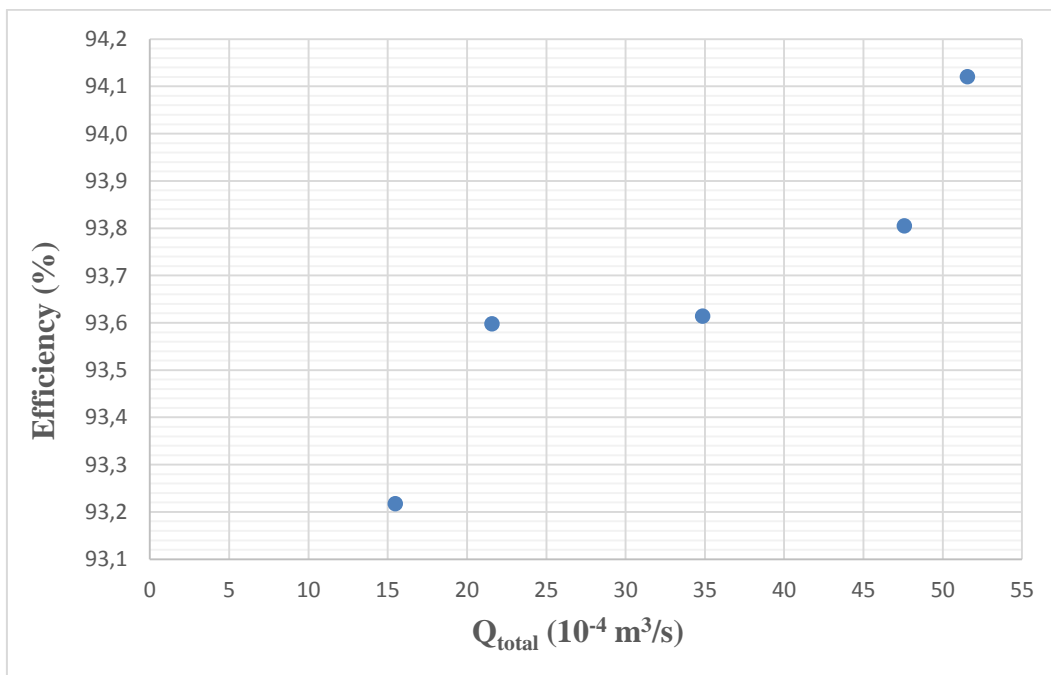
Figure 4.5 Total discharge versus efficiency for $V_R = 44.8$ %

➢ **Case A5:** $V_R = 49.5\%$ (2cm gap – 1 cm full)

The data for Case A5 that are collected for the grated inlet with bar distance of 2 cm gap – 1 cm full ($V_R = 49.5$ %) are presented in Table 4.5 and in Figure 4.6.

Table 4.5 Total discharge and efficiency values for $V_R = 49.5$ %

$Q_t (10^{-4} m^3/s)$	Efficiency (%)
15.768	100.000
22.159	98.264
35.351	98.298
51.041	96.902
52.368	96.578
55.655	96.941
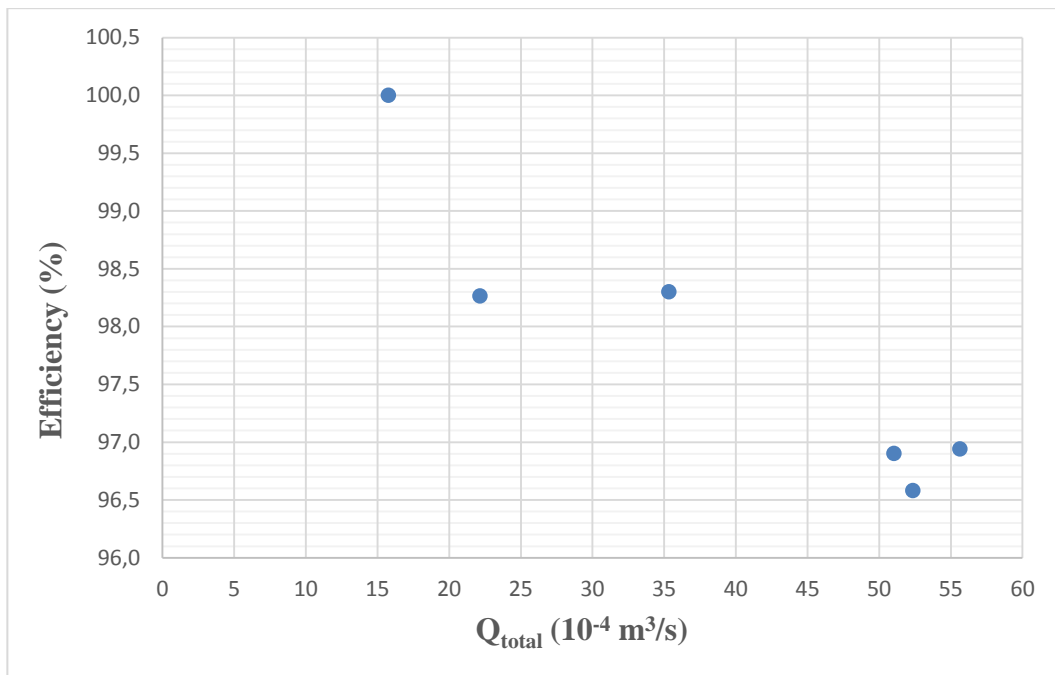
Figure 4.6 Total discharge versus efficiency for $V_R = 49.5$ %

> ➤ **Case A6:** $V_R = 51.22$ % (2.5 cm gap – 1 cm full)

The gathered data for Case A6 that include the grated inlet with bar distance of 2.5 cm gap – 1 cm full ($V_R = 51.22$ %) are illustrated in Table 4.6 and in Figure 4.7.

Table 4.6 Total discharge and efficiency values for $V_R = 51.22$ %

Q_t (10^{-4} m³/s)	Efficiency (%)
21.127	95.559
35.300	95.631
48.476	95.529
50.266	95.442
50.472	95.270
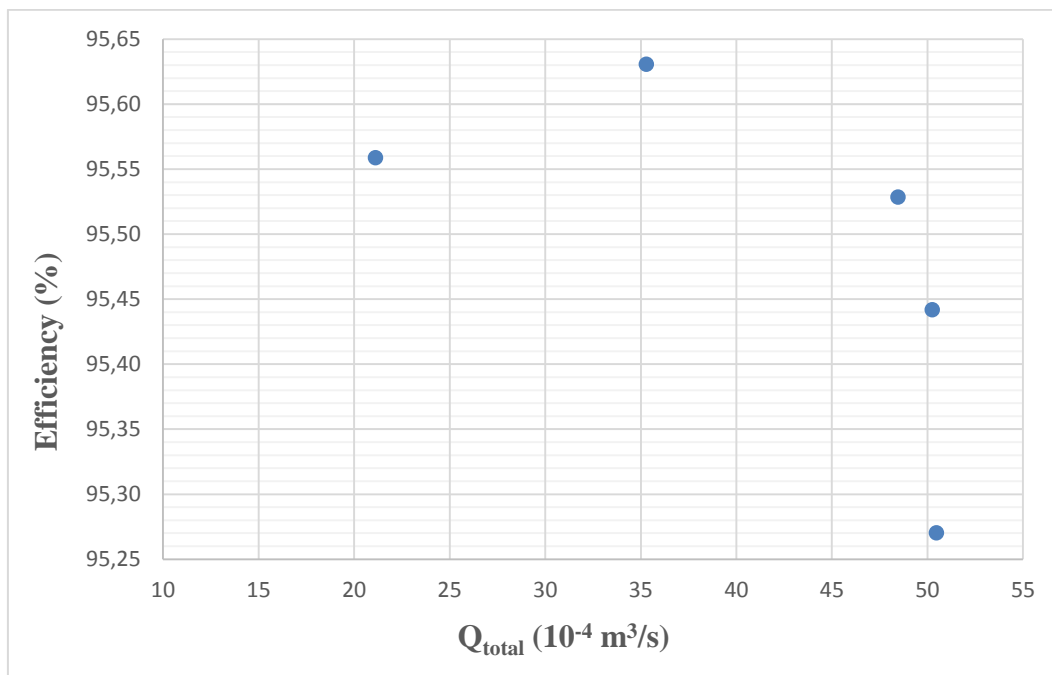
Figure 4.7 Total discharge versus efficiency for $V_R = 51.22$ %

In Figure 4.8 below, all data of six cases are presented in single graphic in order to examine the variations of the efficiency with respect to the total upcoming discharge.
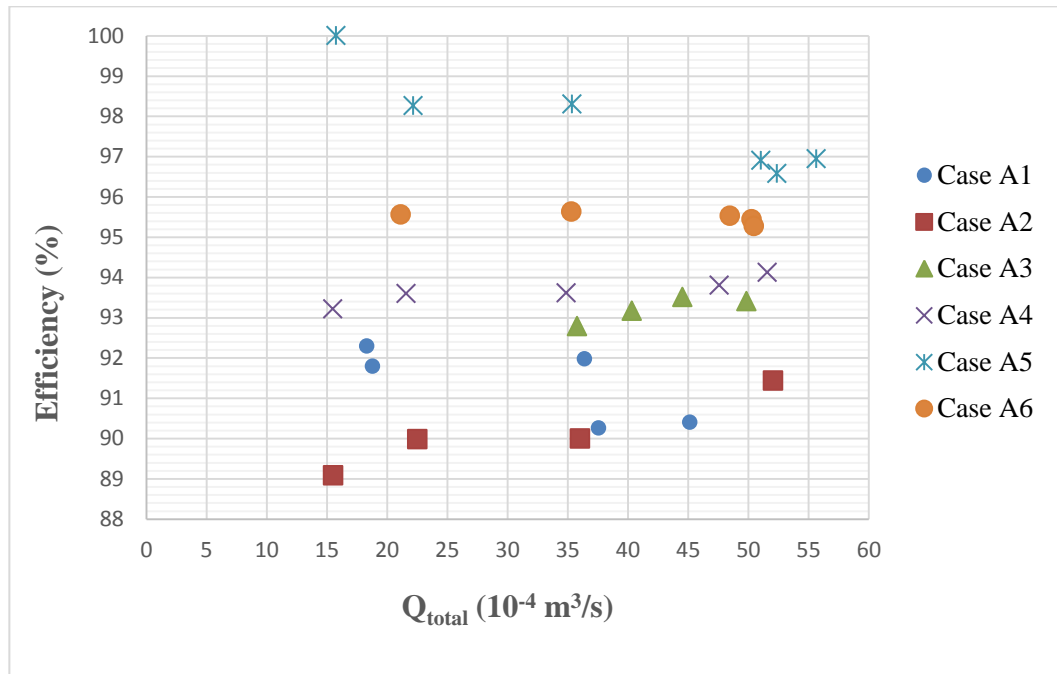
Figure 4.8 Total discharge versus efficiency for all six cases

As displayed in the tables and figures above, the hydraulic efficiency and the corresponding performance of the transverse grated inlets generally show an increasing tendency when the total discharge increases (Tiğrek and Sipahi, 2011). However, it is observed that the curve starts to fall as a declining portion after a certain value of flow rate.

4.1.2. Void Ratio

Considering the above mentioned results, the relationship between the void ratio and the efficiency of grates is studied for particular ranges of discharge values. For this purpose, discharge values of Q_t = 20-25, 35-40 and 50-55 ($10^{-4} \times m^3/s$) are examined respectively in the following tables and graphics.

> **For Q_t = 20–25 ($10^{-4} \times$ m^3/s)**

The efficiencies of the grated inlets depending on the void ratio for the total discharge between Q_t = 20–25 ($10^{-4} \times$ m^3/s) are displayed in Table 4.7 and in Figure 4.9.

Table 4.7 Void ratio and efficiency values for Q_t = 20–25 ($10^{-4} \times$ m^3/s)

Void Ratio (%)	Efficiency (%)
40.55	89.98
44.80	93.60
49.50	98.26
51.22	95.56
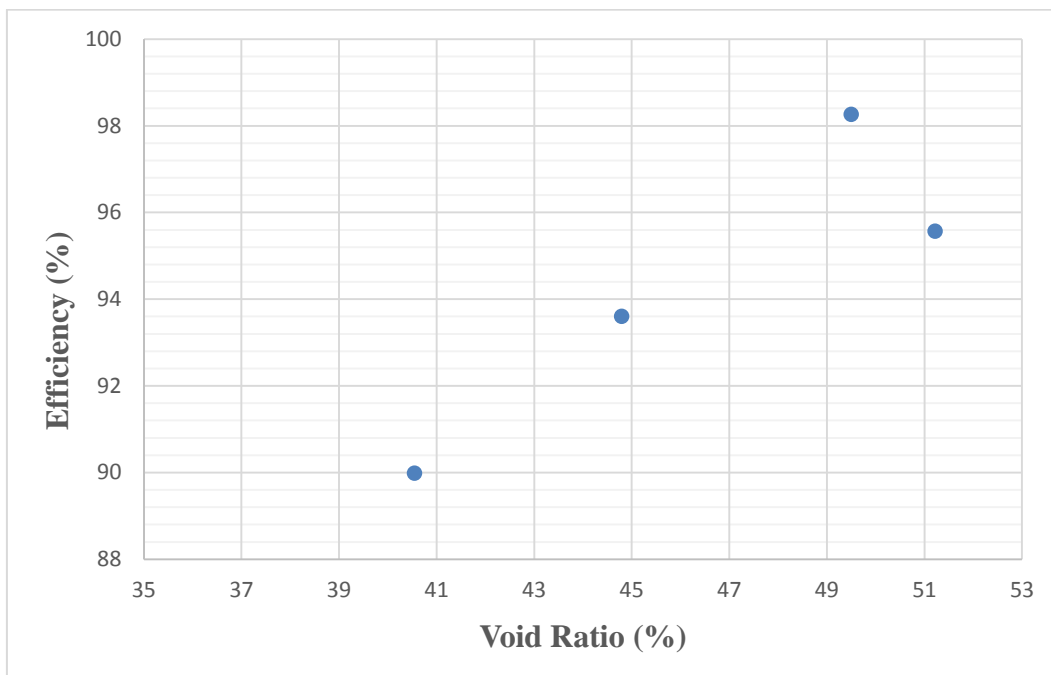
Figure 4.9 Void ratio versus efficiency for Q_t = 20–25 ($10^{-4} \times$ m^3/s)

> **For $Q_t = 35$–40 ($10^{-4} \times$ m³/s)**

The efficiencies of the grated inlets with respect to the void ratio for the total flow rate of $Q_t = 35$–40 ($10^{-4} \times$ m³/s) are listed in Table 4.8 and shown in Figure 4.10.

Table 4.8 Void ratio and efficiency values for $Q_t = 35$–40 ($10^{-4} \times$ m³/s)

Void Ratio (%)	Efficiency (%)
37.56	90.26
37.56	91.98
40.55	90.00
42.60	92.79
49.50	98.30
51.22	95.63
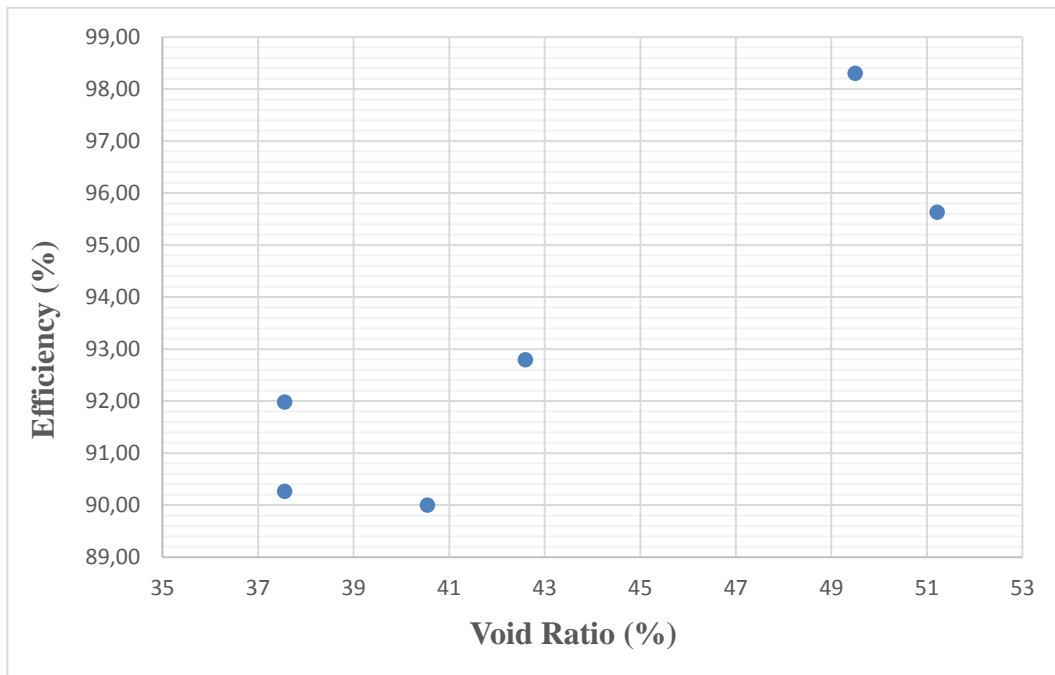
Figure 4.10 Void ratio versus efficiency for $Q_t = 35$–40 ($10^{-4} \times$ m³/s)

➢ **For Q$_t$ = 50–55 (10^{-4} × m^3/s)**

The efficiencies of the grated inlets depending on the void ratio for the total discharge of Q$_t$ = 50–55 (10^{-4} × m^3/s) are presented in Table 4.9 and in Figure 4.11.

Table 4.9 Void ratio and efficiency values for Q$_t$ = 50–55 (10^{-4} × m^3/s)

Void Ratio (%)	Efficiency (%)
40.55	91.44
44.80	94.12
49.50	96.58
49.50	96.90
51.22	95.27
51.22	95.44
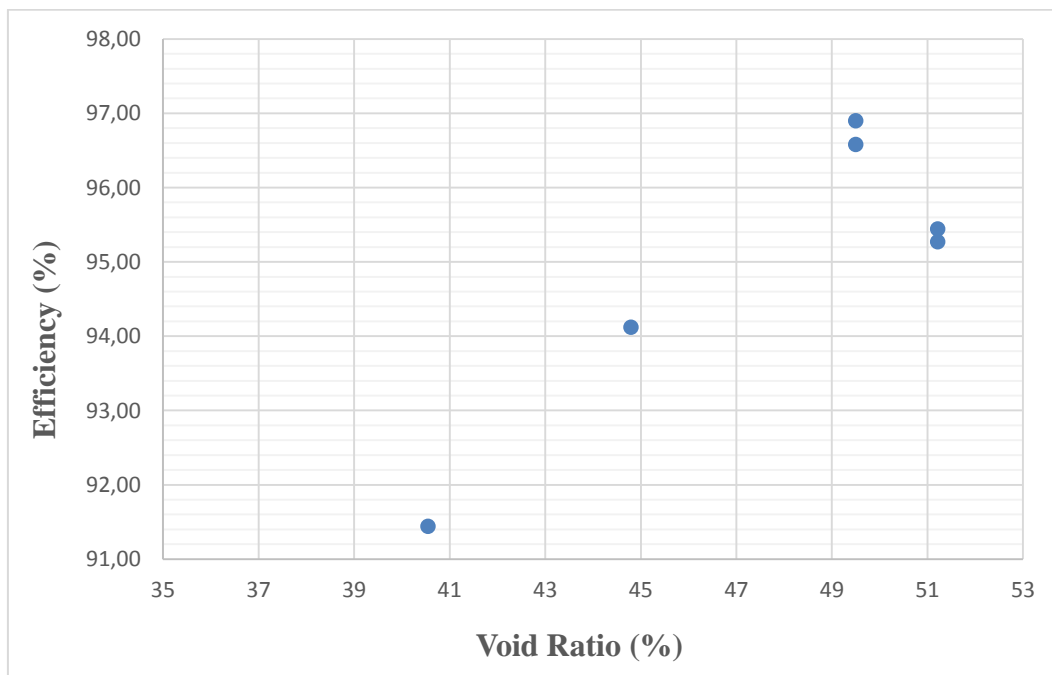
Figure 4.11 Void ratio versus efficiency for Q$_t$ = 50–55 (10^{-4} × m^3/s)

As illustrated in the tables and figures above, for all three different ranges of discharge values, efficiencies of the grated inlets increase with increasing void ratio up to a certain point and then exhibit a declining tendency despite the ongoing increasing void ratio. It is observed that the most efficient grated inlet has the void ratio of 49.50%. In other words, it can be inferred from the data presented in the graphics that the grated inlet having a bar distance of 2 cm gap – 1 cm full (Case A5) has the highest hydraulic efficiency among the six types of grates that are utilized in this current study.

4.1.3. Froude Number

Another parameter that affects the hydraulic efficiency of a grated inlet is the Froude number. While conducting the laboratory experiments, flow depths are measured in each step in order to calculate the corresponding Froude number which was described in Equation 2.9 as,

$$Fr = \frac{Q_t}{\sqrt{9.81b^2 y_1^3}} \tag{2.9}$$

$$Fr = V/\sqrt{gy} \tag{4.1}$$

In Figure 4.12, all the data for the six cases are illustrated with respect to the Froude number considering the total discharges and the related flow depths. Correspondingly, all the values of flow depths for each case are presented in Appendix D.
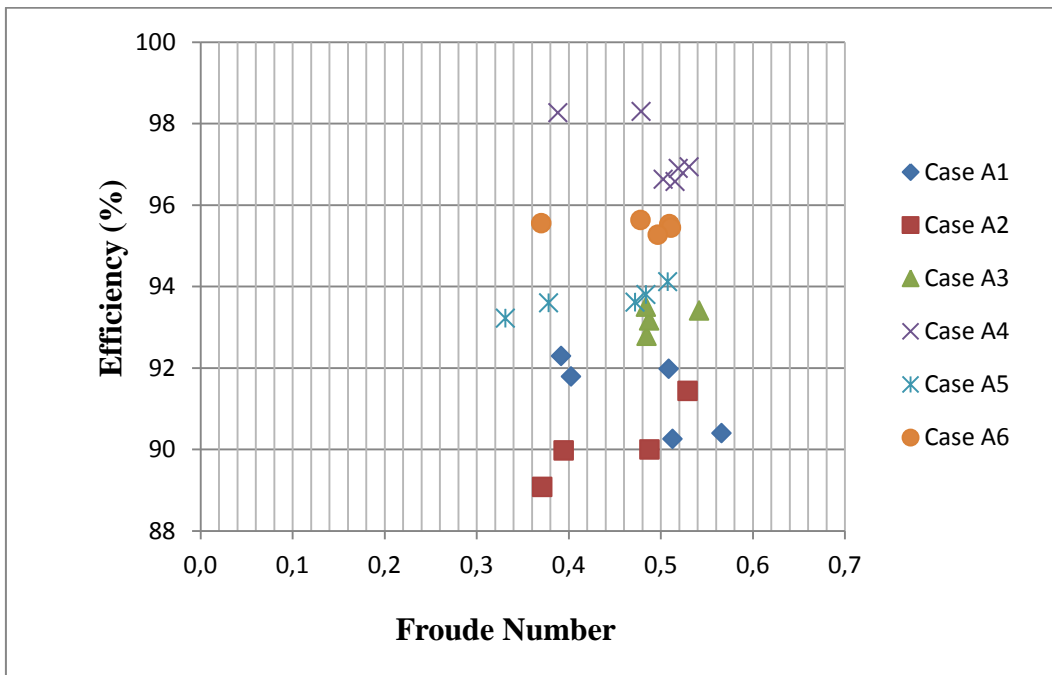
Figure 4.12 Froude number versus efficiency for all six cases

4.2. Total Flow versus Efficiency: Grate Orientation

Second part of the experiments has been performed aiming to observe the effect of grate configuration on the efficiency as well as the interdependence between the efficiency and the distance between the two successive grates that are placed on the main channel.

4.2.1. Grate Configuration

In this part, a specific case has been examined with two different grated inlets, one having grated bars only on the left-hand side and the other having symmetric grated bars on both sides with a specified closed part at the middle. All of the laboratory data for both cases are presented in Appendix B.

Case B1: Grated bars only on the left part

The measured efficiency values of the inlet which has grated bars placed only on the left-hand side are illustrated in Table 4.10 and in Figure 4.13.

Table 4.10 Total discharge and efficiency values for grated bars on the left side

$Q_t (10^{-4} \text{ m}^3/\text{s})$	Efficiency (%)
11.466	64.022
16.112	67.372
22.605	68.711
34.973	70.537
43.127	71.745
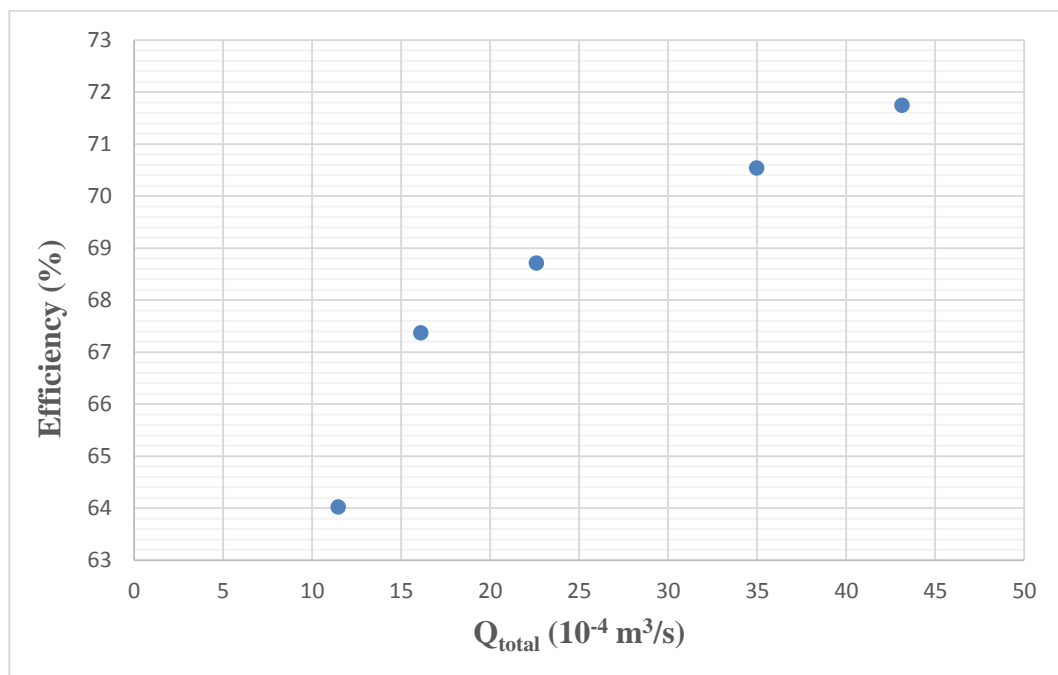
Figure 4.13 Total discharge versus efficiency for grated bars on the left side

➤ **Case B2:** Grated bars on both sides with full middle part

The efficiency values that are computed for the inlet that has grated bars symmetrically placed on both sides are listed in Table 4.11 and are shown in Figure 4.14.

Table 4.11 Total discharge and efficiency values for grated bars on both sides

Q_t (10^{-4} m³/s)	Efficiency (%)
11.775	60.874
18.460	64.727
28.922	69.582
42.637	73.450
46.233	74.202
47.908	74.082
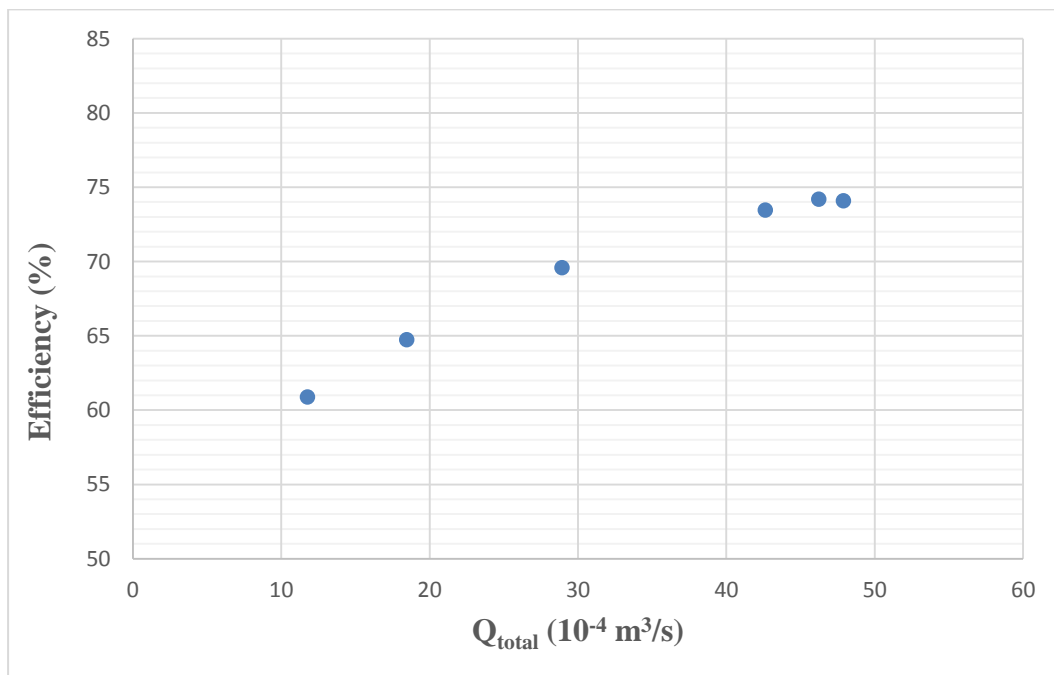
Figure 4.14 Total discharge versus efficiency for grated bars on both sides

4.2.2. Comparison of Three Cases

Considering the two grate configuration cases above, efficiencies of the three cases are compared for a specific constant total discharge value varying between 15 and 40 (10^{-4} m^3/s). The obtained values for the efficiencies of these cases are displayed in Table 4.12 and in Figure 4.15.

Table 4.12 Comparison of efficiencies in terms of configuration

Discharge (10^{-4} m^3/s)	Efficiency (%) Case B1	Efficiency (%) Case B2	Efficiency (%) Case A1
20	68.23	65.50	91,78
25	69.10	68.00	91,90
30	69.80	69.90	92,01
35	70.55	71.40	92,04
40	71.30	72.80	90,18
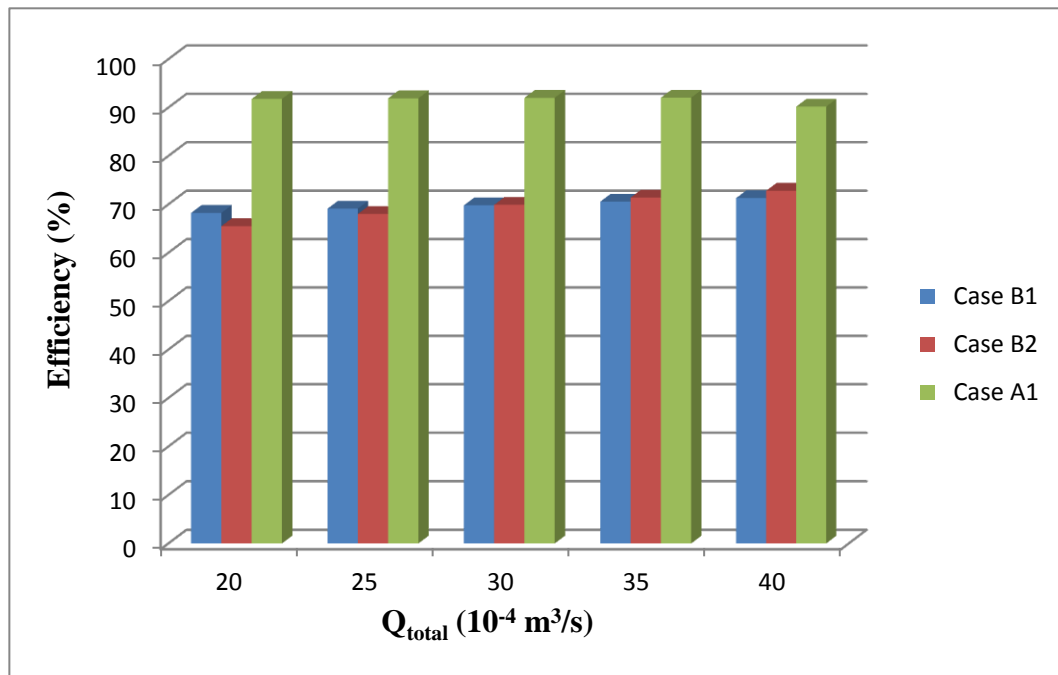
Figure 4.15 Configuration versus efficiency for Case B1, Case B2 and Case A1 for varying discharge values

Table 4.12 and Figure 4.15 illustrate that the data concerning the efficiency of the inlet system having grated bars only on the left part (Case B1) and the inlet system having grated bars on both ends (Case B2) is almost similar. However, Case B1 indicates a slightly higher efficiency for lower rates of flows whereas Case B2 shows a slight hydraulic advantage for higher rates of flows. On the contrary, the results of this experiment indicate that the hydraulic efficiency of the continuous grate inlet is considerably higher for all discharge values when it is compared to other two cases.

The above mentioned experiment for grate configuration is conducted by gathering of several data with their replications. However, handling the whole experiment by just one researcher, performing them for the first time at METU Hydromechanics Laboratory setup and also due to the lack of studies in the literature concerning this issue prevented these results to be enhanced and to be more generalizable.

4.3. Total Flow versus Efficiency: Distance between Grates

4.3.1. Distance between Grates

In this part, the influence of the distance between two successive grated inlets on the hydraulic efficiency is investigated by means of the laboratory experiments. While conducting the tests, inlets that have grated bars only on the left-hand side and bars only on the right-hand side are utilized. The gathered laboratory data for the two cases are fully presented in Appendix C.

➢ **Case C1**: Successive Grates at Section (1) and Section (2)

The calculated efficiencies for the first case which includes successive grates placed at section (1) and section (2) are presented in Table 4.13 and are shown in Figure 4.16.

Table 4.13 Total discharge and efficiency values for grates at section (1) and (2)

Q_t (10^{-4} m^3/s)	Efficiency (%)
11.567	71.224
15.805	72.891
22.915	74.914
34.886	77.084
47.407	78.973
50.917	78.938
51.563	78.473
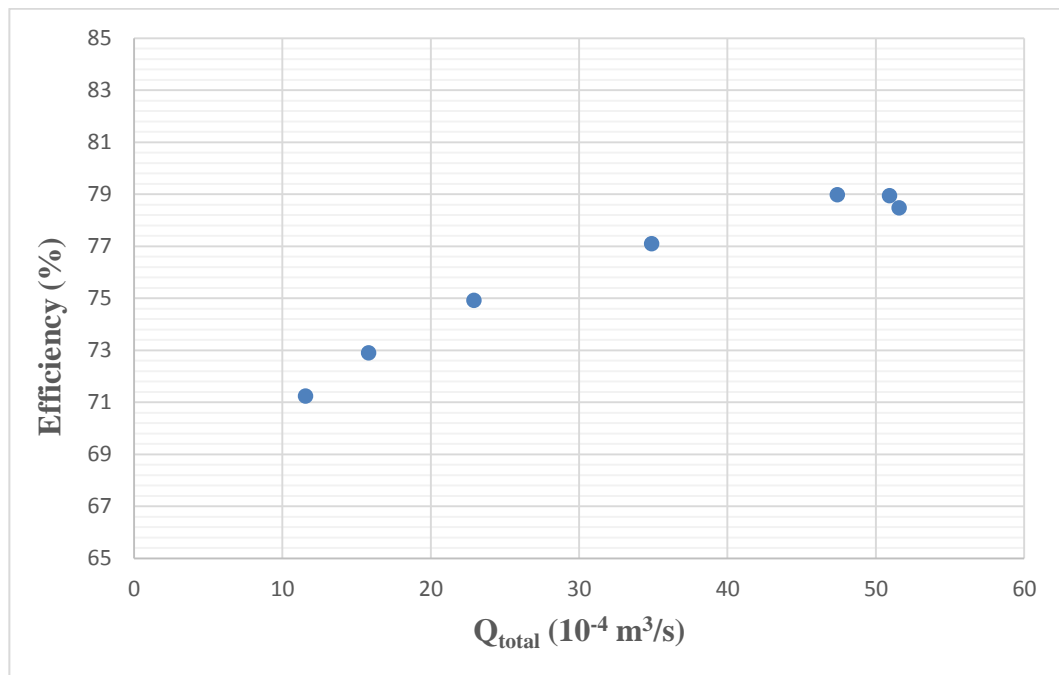
Figure 4.16 Total discharge versus efficiency for grates at section (1) and section (2)

> ➤ **Case C2:** Successive Grates at Section (1) and Section (3)

The efficiencies that are computed for the second case including successive grates at

section (1) and section (3) are listed in Table 4.14 and are shown in Figure 4.17.

Table 4.14 Total discharge and efficiency values for grates at section (1) and (3)

Q_t (10^{-4} m^3/s)	Efficiency (%)
12.005	68.204
14.261	69.943
16.252	70.830
18.251	72.300
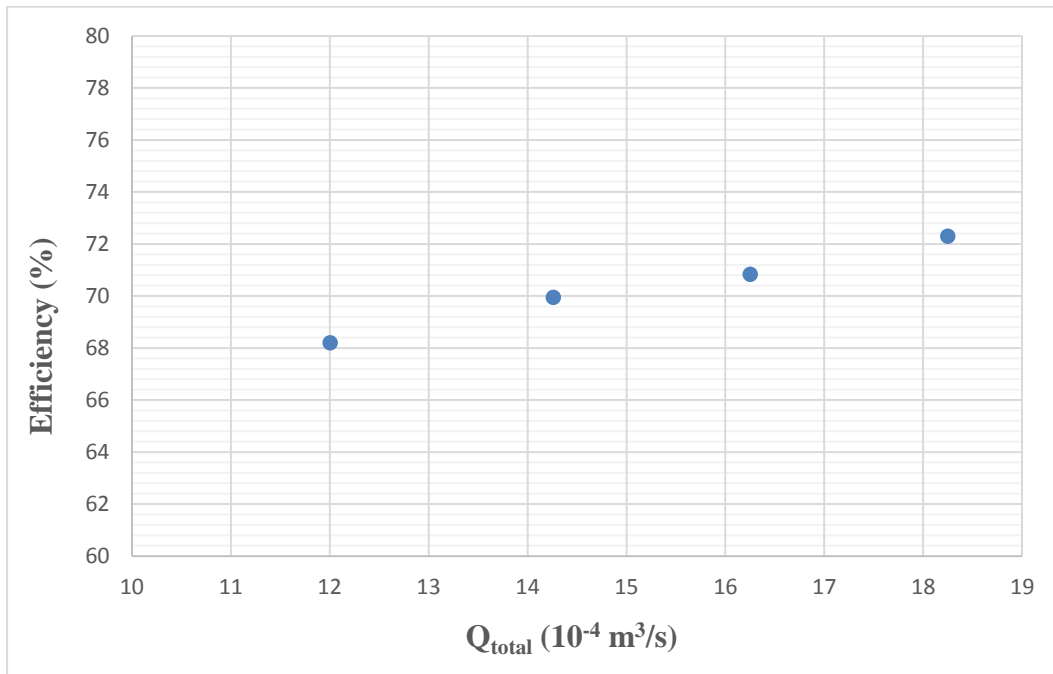
Figure 4.17 Total discharge versus efficiency for grates at section (1) and section (3)

4.3.2. Comparison of Two Cases

The distance between two consecutive grates is taken into consideration and comparison of the efficiencies is shown graphically. Similarly, this is fulfilled by keeping the total discharge value constant each time, ranging between 12 and 18

(10^{-4} m^3/s). Corresponding values of the grate efficiencies are listed in Table 4.15 and are illustrated in Figure 4.18.

Table 4.15 Comparison of efficiencies in terms of distance between grates

Discharge (10^{-4} m^3/s)	Efficiency (%) Case C1	Efficiency (%) Case C2
12	71.40	68.20
14	72.22	69.78
16	72.96	70.70
18	73.60	72.10
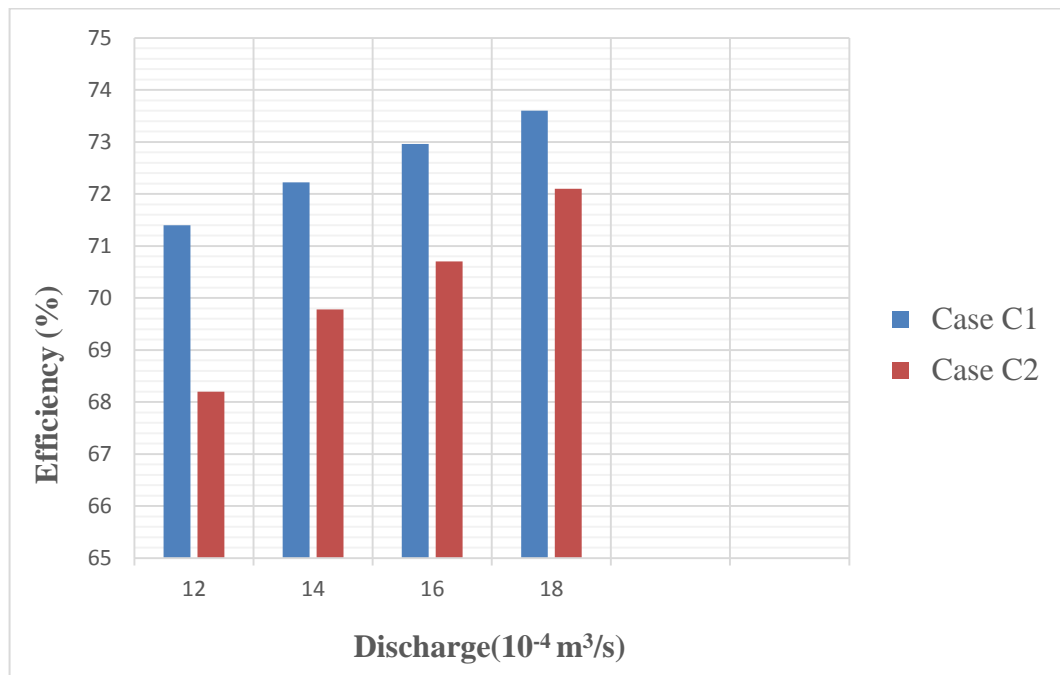
Figure 4.18 Distance between grates versus efficiency for Case C1 and Case C2 for varying discharge values

As presented in Figure 4.18, the hydraulic performance of the system in which two successive grates are placed at section (1) and (2) is superior to the case having grates at section (1) and (3). In other words, it can be inferred that placing two sequential grates for relatively lesser distance provides a higher efficiency in

intercepting the upcoming total flow when compared to a system having larger grate intervals.

CHAPTER 5

CONCLUSION

In this study, the efficiency of grated inlets has been investigated by conducting laboratory experiments in order to examine the factors affecting the hydraulic efficiency of the inlet systems. Moreover, the relationship between the total approaching flow and the grate efficiency has been observed with regard to certain parameters. Although hydraulic performance and the corresponding efficiency of a grate depend on several parameters such as longitudinal and cross slope of the roads, total approaching flow, roughness of the pavements, geometrical and configurational conditions of the grates and clogging factors, in the present study grate dimensions and configuration together with variable discharge was concern due to limitations of laboratory facilities. Thus, outcomes of the study can be listed as follows;

1. It has been observed from the experiments that there exist a close interdependence between the total flow rate and the grate efficiency and it has been also revealed that the hydraulic efficiency increases when the total flow increases as well. Nevertheless, after a certain point, degradation of efficiency occurs despite the progressing increase in the total flow rate.

2. When void ratio is taken into consideration, the inlet having 1 cm bars and 2 cm spacing is hydraulically the most efficient grate and it corresponds to a void ratio of 49.5%.

3. Hydraulic performance of the grate systems and the corresponding grate efficiency are influenced by various configurations of the grates such as having grates on both sides or on one side of the road.

4. The distance between the two successive grate inlets also affects the performance and the efficiency of an inlet. According to the conducted experiments, when the grates are placed closer to each other, the system becomes hydraulically more efficient in capturing the upcoming water.

5. Finally, in future studies, longitudinal slope and roughness of the main channel could also be taken into consideration while examining the interdependence between the total discharge and the grate efficiency with respect to void ratio or different grate orientations.

REFERENCES

American Society of Civil Engineers (1960). *Design manual for storm drainage.* New York.

Bauer, W. J., & Woo, D. C. (1964). Hydraulic design of depressed curb-opening inlets. *Highway Research Record*, (58), 61-80.

Chow, V. T. (1959). *Open-channel hydraulics.* New York: Mc-Graw-Hill.

Comport, B. C., & Thornton, C. I. (2012). Hydraulic efficiency of grate and curb inlets for urban storm drainage. *Journal of Hydraulic Engineering, 138*(10), 878-884.

Fang, X., Jiang, S., & Alam, S. R. (2010). Numerical simulations of efficiency of curb-opening inlets. *Journal of Hydraulic Engineering, 136*(1), 62-66. doi: 10.1061/ASCEHY.1943-7900.0000131

Fujita, S. (2002, September). *A scenario for the modernization of urban drainage.* 9th International Conference on Urban Drainage–Global Solutions for Urban Drainage, Oregon, USA.

Gomez, M., & Russo, B. (2005, August). *Comparative study among different methodologies to determine storm sewer inlet efficiency from test data.* 10th international conference on urban drainage, Copenhagen, Denmark.

Gomez, M., & Russo, B. (2009). Hydraulic efficiency of continuous transverse grates for paved areas. *Journal of Irrigation and Drainage Engineering, 135*(2), 225-230.

Gomez M, Russo B (2010) Methodology to estimate hydraulic efficiency of drain inlets. *Water Management-ICE*, 1–10.

Guo, J. C., MacKenzie, K. A., & Mommandi, A. (2009). Design of street sump inlet. *Journal of Hydraulic Engineering, 135*(11), 1000-1004. doi: 10.1061/(ASCE)HY.1943-7900.0000094

Hammonds, M. A., & Holley, E. (1995). *Hydraulic Characteristics of Flush Depressed Curb Inlets and Bridge Deck Drains*. Texas.

HEC-22, U.S. Army Corps. of Engineers, (1991). *Urban Drainage Design Manual, Hydraulic Engineering Circular 22*. Colorado.

Huebner, R. S., Reed, J. R., & Henry, J. J. (1986). Criteria for predicting hydroplaning potential. *Journal of Transportation Engineering, 112*(5), 549-553.

Izzard, C. F. (1950). *Tentative Results on Capacity of Curb Opening Inlets (Report No. 11-13)*, Washington, D.C: Highway Research Board.

Jiang, S. (2007). *Numerical simulations of shallow flow through curb-opening inlets at various longitudinal and cross slopes*. Lamar University-Beaumont.

Jones, J. (2006) Residential Stormwater Management. Great Works on Urban Water Resources (1962-2001): pp. 649-704. doi 10.1061/9780784408438.ch23.

Mustaffa, Z. (2003). *An experimental investigation of the hydraulics of street inlets* (Unpublished doctoral dissertation). Universiti Teknologi, Petronas.

Nicklow, J. W., & Hellman, A. P. (2000). Optimizing hydraulic design of highway drainage systems. *Building Partnerships*, 1-10. doi: 10.1061/40517(2000)175

Pazwash, H. and Boswell, S. (2003). Proper design of inlets and drains for roadways and urban developments. *World Water & Environmental Resources Congress 2003,* 1-10. doi: 10.1061/40685(2003)304

Russo, B., Gómez, M., & Tellez, J. (2013). Methodology to estimate the hydraulic efficiency of nontested continuous transverse grates. *Journal of Irrigation and Drainage Engineering, 139*(10), 864-871. doi: 10.1061/(ASCE)IR.1943-4774.0000625.

Sezenöz, B. (2014). *Numerical modelling of continuous transverse grates for hydraulic efficiency* (Unpublished master's thesis). Middle East Technical University, Ankara.

Sipahi S.Ö. (2006). *Calibration of a grate on a sloping channel* (Unpublished master's thesis). Middle East Technical University, Ankara.

Şahin, H. İ. (2006). *Examination of grate inlets within urban stormwater drainage* (Unpublished master's thesis). İstanbul Technical University, İstanbul.

Tiğrek, Ş., & Sipahi, S. Ö. (2011). Rehabilitation of storm water collection systems of urban environment using the small roads as conveyance channels. *International Journal of Environmental Science and Technology*, *9*(1), 95-103.

Uyumaz, A. (1992). Discharge capacity for curb-opening inlets. *Journal of Hydraulic Engineering, 118*(7), 1048-1051.

APPENDIX A

VOID RATIO

Table A.1 Discharge values for 2 cm gap – 2 cm full system

Time (sec)	Increase in Pool 1 (cm)	Q_i (lt/s)
10.8	2.0	1.814815
26.5	4.6	1.701132
48.1	8.3	1.691060
89.5	14.7	1.609609
151.4	25.2	1.631176
		1.689558

Time (sec)	Increase in Bypass Pool (cm)	Q_b (lt/s)
108.0	1.5	0.136111
277.7	4.0	0.141160
559.0	8.2	0.143757
956.3	14.0	0.143470
1491.7	21.5	0.141248
		0.141149

Time (sec)	Increase in Pool 1 (cm)	Q_i (lt/s)
10.6	2.0	1.849057
27.7	4.6	1.627437
47.8	8.3	1.701674
83.3	14.7	1.729412
143.3	25.2	1.723378
		1.726191

Time (sec)	Increase in Bypass Pool (cm)	Q_b (lt/s)
93.4	1.5	0.157388
262.7	4.0	0.149220
513.4	8.2	0.156525
979.6	15.5	0.155063
1370.2	21.5	0.153773
		0.154394

Time (sec)	Increase in Pool 1 (cm)	Q_i (lt/s)
5.5	2.0	3.563636
12.7	4.6	3.549606
23.7	8.3	3.432068
42.0	14.7	3.430000
74.8	25.2	3.301604
		3.455383

Time (sec)	Increase in Bypass Pool (cm)	Q_b (lt/s)
49.3	1.5	0.298174
131.0	4.0	0.299237
265.9	8.2	0.302219
452.5	14.0	0.303204
692.3	21.5	0.304348
		0.301436

Table A.1 (continued)

Time (sec)	Increase in Pool 1 (cm)	Q_i (lt/s)
6.0	2.0	3.266667
13.6	4.6	3.314706
24.5	8.3	3.320000
43.5	14.7	3.311724
76.9	25.2	3.211443
		3.284908

Time (sec)	Increase in Bypass Pool (cm)	Q_b (lt/s)
44.2	1.5	0.332579
110.3	4.0	0.355394
220.6	8.2	0.364279
379.8	14.0	0.361243
585.9	21.5	0.359618
		0.354623

Time (sec)	Increase in Pool 1 (cm)	Q_i (lt/s)
4.1	2.0	4.780488
11.2	4.6	4.025000
21.2	8.3	3.836792
36.2	14.7	3.979558
65.3	25.2	3.781930
		4.080754

Time (sec)	Increase in Bypass Pool (cm)	Q_b (lt/s)
35.6	1.5	0.412921
90.4	4.0	0.433628
181.5	8.2	0.442755
310.8	14.0	0.441441
483.4	21.5	0.435871
		0.433323

Table A.2 Discharge values for 2.5 cm gap – 2 cm full system

Time (sec)	Increase in Pool 1 (cm)	Q_i (lt/s)
14.4	2.0	1.361111
32.2	4.6	1.400000
59.7	8.3	1.362479
102.8	14.7	1.401362
177.7	25.2	1.389758
		1.382942

Time (sec)	Increase in Bypass Pool (cm)	Q_b (lt/s)
86.3	1.5	0.170336
232.5	4.0	0.168602
473.5	8.2	0.169715
		0.169551

Table A.2 (continued)

Time (sec)	Increase in Pool 1 (cm)	Q_i (lt/s)
9.5	2.0	2.063158
22.0	4.6	2.049091
39.8	8.3	2.043719
71.4	14.7	2.017647
126.0	25.2	1.960000
		2.026723

Time (sec)	Increase in Bypass Pool (cm)	Q_b (lt/s)
66.0	1.5	0.222727
174.5	4.0	0.224642
349.5	8.2	0.229928
		0.225766

Time (sec)	Increase in Pool 1 (cm)	Q_i (lt/s)
6.1	2.0	3.213115
13.7	4.6	3.290511
25.3	8.3	3.215020
43.7	14.7	3.296568
77.2	25.2	3.198964
		3.242835

Time (sec)	Increase in Bypass Pool (cm)	Q_b (lt/s)
40.7	1.5	0.361179
109.6	4.0	0.357664
221.7	8.2	0.362472
381.1	14.0	0.360010
		0.360331

Time (sec)	Increase in Pool 1 (cm)	Q_i (lt/s)
22.8	10.5	4.513158
21.8	10.5	4.720183
12.6	6.4	4.977778
34.3	16.9	4.828571
		4.759923

Time (sec)	Increase in Bypass Pool (cm)	Q_b (lt/s)
33.4	1.5	0.440120
88.5	4.0	0.442938
176.8	8.2	0.454525
307.6	14.0	0.446034
		0.445904

Table A.3 Discharge values for 2 cm gap – 1.5 cm full system

Time (sec)	Increase in Pool 1 (cm)	Q_i (lt/s)
5.6	2.0	3.500000
13.9	4.6	3.243165
25.1	8.3	3.240637
43.5	14.7	3.311724
74.6	25.2	3.310456
		3.321197

Time (sec)	Increase in Bypass Pool (cm)	Q_b (lt/s)
57.2	1.5	0.256993
152.9	4.0	0.256377
307.9	8.2	0.260994
		0.258121

Time (sec)	Increase in Pool 1 (cm)	Q_i (lt/s)
5.5	2.0	3.563636
11.9	4.6	3.788235
21.6	8.3	3.765741
37.4	14.7	3.851872
64.6	25.2	3.822910
		3.758479

Time (sec)	Increase in Bypass Pool (cm)	Q_b (lt/s)
53.0	1.5	0.277358
143.3	4.0	0.273552
291.0	8.2	0.276151
		0.275687

Time (sec)	Increase in Pool 1 (cm)	Q_i (lt/s)
4.3	2.0	4.558140
10.9	4.6	4.135780
20.4	8.3	3.987255
35.7	14.7	4.035294
60.1	25.2	4.109151
		4.165124

Time (sec)	Increase in Bypass Pool (cm)	Q_b (lt/s)
50.4	1.5	0.291667
136.3	4.0	0.287601
278.4	8.2	0.288649
		0.289306

Table A.3 (continued)

Time (sec)	Increase in Pool 1 (cm)	Q_i (lt/s)
3.9	2.0	5.025641
9.7	4.6	4.647423
18.1	8.3	4.493923
31.7	14.7	4.544479
54.1	25.2	4.564880
		4.655269

Time (sec)	Increase in Bypass Pool (cm)	Q_b (lt/s)
45.5	1.5	0.323077
117.5	4.0	0.333617
244.4	8.2	0.328805
		0.328500

Table A.4 Discharge values for 2.5 cm gap − 1.5 cm full system

Time (sec)	Increase in Pool 1 (cm)	Q_i (lt/s)
13.3	2.0	1.473684
31.0	4.6	1.454194
57.5	8.3	1.414609
99.8	14.7	1.443487
172.6	25.2	1.430823
		1.443359

Time (sec)	Increase in Bypass Pool (cm)	Q_b (lt/s)
138.5	1.5	0.106137
216.9	2.3	0.103919
		0.105028

Time (sec)	Increase in Pool 1 (cm)	Q_i (lt/s)
9.6	2.0	2.041667
22.2	4.6	2.030631
40.3	8.3	2.018362
71.4	14.7	2.017647
124.1	25.2	1.990008
		2.019663

Time (sec)	Increase in Bypass Pool (cm)	Q_b (lt/s)
104.3	1.5	0.140940
166.5	2.3	0.135375
		0.138157

Table A.4 (continued)

Time (sec)	Increase in Pool 1 (cm)	Q_i (lt/s)
5.9	2.0	3.322034
14.0	4.6	3.220000
25.0	8.3	3.253600
43.7	14.7	3.296568
76.5	25.2	3.228235
		3.264087

Time (sec)	Increase in Bypass Pool (cm)	Q_b (lt/s)
67.4	1.5	0.218101
175.4	4.0	0.223489
354.9	8.2	0.226430
		0.222673

Time (sec)	Increase in Pool 1 (cm)	Q_i (lt/s)
23.0	10.5	4.473913
23.1	10.5	4.454545
		4.464229

Time (sec)	Increase in Bypass Pool (cm)	Q_b (lt/s)
49.6	1.5	0.296371
134.9	4.0	0.290586
270.1	8.2	0.297519
		0.294825

Time (sec)	Increase in Pool 1 (cm)	Q_i (lt/s)
21.0	10.5	4.900000
21.4	10.5	4.808411
		4.854206

Time (sec)	Increase in Bypass Pool (cm)	Q_b (lt/s)
48.4	1.5	0.303719
130.7	4.0	0.299923
262.5	8.2	0.306133
		0.303259

Table A.5 Discharge values for 2 cm gap – 1 cm full system

Time (sec)	Increase in Pool 1 (cm)	Q_i (lt/s)
12.4	2.0	1.580645
28.4	4.6	1.587324
51.9	8.3	1.567245
90.8	14.7	1.586564
158.1	25.2	1.562049
		1.576765

Time (sec)	Increase in Bypass Pool (cm)	Q_b (lt/s)
30	0	0
		0

Time (sec)	Increase in Pool 1 (cm)	Q_i (lt/s)
8.9	2.0	2.202247
20.3	4.6	2.220690
37.3	8.3	2.180697
66.8	14.7	2.156587
116.1	25.2	2.127132
		2.177471

Time (sec)	Increase in Bypass Pool (cm)	Q_b (lt/s)
585.8	2.3	0.038477
		0.038477

Time (sec)	Increase in Pool 1 (cm)	Q_i (lt/s)
5.5	2.0	3.563636
13.0	4.6	3.467692
23.1	8.3	3.521212
41.5	14.7	3.471325
73.7	25.2	3.350882
		3.474950

Time (sec)	Increase in Bypass Pool (cm)	Q_b (lt/s)
243.0	1.5	0.060494
376.8	2.3	0.059820
		0.060157

Table A.5 (continued)

Time (sec)	Increase in Pool 1 (cm)	Q_i (lt/s)
3.9	2.0	5.025641
9.3	4.6	4.847312
16.1	8.3	5.052174
29.2	14.7	4.933562
50.7	25.2	4.871006
		4.945939

Time (sec)	Increase in Bypass Pool (cm)	Q_b (lt/s)
92.9	1.5	0.158235
142.6	2.3	0.158065
		0.158150

Time (sec)	Increase in Pool 1 (cm)	Q_i (lt/s)
3.8	2.0	5.157895
8.8	4.6	5.122727
16.2	8.3	5.020988
28.6	14.7	5.037063
49.9	25.2	4.949098
		5.057554

Time (sec)	Increase in Bypass Pool (cm)	Q_b (lt/s)
81.5	1.5	0.180368
126.6	2.3	0.178041
		0.179205

Time (sec)	Increase in Pool 1 (cm)	Q_i (lt/s)
3.4	2.0	5.764706
8.2	4.6	5.497561
15.1	8.3	5.386755
27.8	14.7	5.182014
48.0	25.2	5.145000
		5.395207

Time (sec)	Increase in Bypass Pool (cm)	Q_b (lt/s)
87.8	1.5	0.167426
130.2	2.3	0.173118
		0.170272

Table A.6 Discharge values for 2.5 cm gap – 1 cm full system

Time (sec)	Increase in Pool 1 (cm)	Q_i (lt/s)
9.5	2.0	2.063158
21.7	4.6	2.077419
40.8	8.3	1.993627
73.0	14.7	1.973425
124.3	25.2	1.986806
		2.018887

Time (sec)	Increase in Bypass Pool (cm)	Q_b (lt/s)
155.4	1.5	0.094595
242.2	2.3	0.093064
		0.093829

Time (sec)	Increase in Pool 1 (cm)	Q_i (lt/s)
5.8	2.0	3.379310
13.2	4.6	3.415152
23.9	8.3	3.403347
42.8	14.7	3.365888
74.5	25.2	3.314899
		3.375719

Time (sec)	Increase in Bypass Pool (cm)	Q_b (lt/s)
96.2	1.5	0.152807
144.8	2.3	0.155663
		0.154235

Time (sec)	Increase in Pool 1 (cm)	Q_i (lt/s)
4.1	2.0	4.780488
9.7	4.6	4.647423
18.2	8.3	4.469231
31.1	14.7	4.632154
53.4	25.2	4.624719
		4.630803

Time (sec)	Increase in Bypass Pool (cm)	Q_b (lt/s)
67.2	1.5	0.218750
182.1	4.0	0.215266
371.6	8.2	0.216254
		0.216757

Time (sec)	Increase in Pool 1 (cm)	Q_i (lt/s)
21.3	10.5	4.830986
21.6	10.5	4.763889
		4.797437

Time (sec)	Increase in Bypass Pool (cm)	Q_b (lt/s)
65.0	1.5	0.226154
171.1	4.0	0.229106
346.2	8.2	0.232120
		0.229127

Table A.6 (continued)

Time (sec)	Increase in Pool 1 (cm)	Q_i (lt/s)		Time (sec)	Increase in Bypass Pool (cm)	Q_b (lt/s)
21.5	10.5	4.786047		61.0	1.5	0.240984
21.3	10.5	4.830986		165.2	4.0	0.237288
		4.808516		337.8	8.2	0.237892
						0.238721

APPENDIX B

CONFIGURATION OF GRATES

Table B.1 Discharge values for grated bars only on the left part

> For Q_t = 1.147 lt/s

Time (sec)	Increase in Pool 1 (cm)	Q_i (lt/s)	Time (sec)	Increase in Bypass Pool (cm)	Q_b (lt/s)
31.0	2.0	0.632258	37.8	1.5	0.388889
63.5	4.6	0.709921	97.5	4.0	0.402051
108.2	8.3	0.751756	191.2	8.2	0.420293
185.5	14.7	0.776604	320.5	14.0	0.428081
308.8	25.2	0.799741	497.8	21.5	0.423262
		0.734056			**0.412515**

> For Q_t = 1.611 lt/s

Time (sec)	Increase in Pool 1 (cm)	Q_i (lt/s)	Time (sec)	Increase in Bypass Pool (cm)	Q_b (lt/s)
16.9	2.0	1.159763	31.7	1.5	0.463722
41.8	4.6	1.078469	76.0	4.0	0.515789
76.1	8.3	1.068857	146.6	8.2	0.548158
136.0	14.7	1.059265	248.0	14.0	0.553226
232.7	25.2	1.061281	384.7	21.5	0.547700
		1.085527			**0.525719**

Table B.1 (continued)

➢ For Q_t = 2.260 lt/s

Time (sec)	Increase in Pool 1 (cm)	Q_i (lt/s)	Time (sec)	Increase in Bypass Pool (cm)	Q_b (lt/s)
12.9	2.0	1.519380	22.3	1.5	0.659193
28.1	4.6	1.604270	55.8	4.0	0.702509
52.3	8.3	1.555258	110.4	8.2	0.727899
92.3	14.7	1.560780	188.3	14.0	0.728625
161.8	25.2	1.526329	293.4	21.5	0.718132
		1.553203			**0.707271**

➢ For Q_t = 3.497 lt/s

Time (sec)	Increase in Pool 1 (cm)	Q_i (lt/s)	Time (sec)	Increase in Bypass Pool (cm)	Q_b (lt/s)
8.0	2.0	2.450000	14.5	1.5	1.013793
18.3	4.6	2.463388	39.0	4.0	1.005128
32.7	8.3	2.487462	76.7	8.2	1.047718
58.0	14.7	2.483793	130.6	14.0	1.050536
100.8	25.2	2.450000	203.6	21.5	1.034872
		2.466929			**1.030410**

➢ For Q_t = 4.313 lt/s

Time (sec)	Increase in Pool 1 (cm)	Q_i (lt/s)	Time (sec)	Increase in Bypass Pool (cm)	Q_b (lt/s)
5.9	2.0	3.322034	12.2	1.5	1.204918
14.8	4.6	3.045946	32.2	4.0	1.217391
26.5	8.3	3.069434	65.9	8.2	1.219423
47.0	14.7	3.065106	111.2	14.0	1.233813
83.2	25.2	2.968269	173.1	21.5	1.217215
		3.094158			**1.218552**

Table B.2 Discharge values for grated bars on both sides

> For Q_t = 1.118 lt/s

Time (sec)	Increase in Pool 1 (cm)	Q_i (lt/s)	Time (sec)	Increase in Bypass Pool (cm)	Q_b (lt/s)
28.5	2.0	0.687719	32.3	1.5	0.455108
63.3	4.6	0.712164	85.2	4.0	0.460094
112.5	8.3	0.723022	173.8	8.2	0.462371
198.1	14.7	0.727208	294.3	14.0	0.466191
336.5	25.2	0.733908	458.2	21.5	0.459843
		0.716804			**0.460721**

> For Q_t = 1.846 lt/s

Time (sec)	Increase in Pool 1 (cm)	Q_i (lt/s)	Time (sec)	Increase in Bypass Pool (cm)	Q_b (lt/s)
16.4	2.0	1.195122	22.5	1.5	0.653333
38.0	4.6	1.186316	60.5	4.0	0.647934
67.9	8.3	1.197938	121.7	8.2	0.660312
119.0	14.7	1.210588	210.0	14.0	0.653333
208.5	25.2	1.184460	328.8	21.5	0.640815
		1.194885			**0.651146**

> For Q_t = 2.892 lt/s

Time (sec)	Increase in Pool 1 (cm)	Q_i (lt/s)	Time (sec)	Increase in Bypass Pool (cm)	Q_b (lt/s)
10.0	2.0	1.960000	16.4	1.5	0.896341
22.0	4.6	2.049091	44.8	4.0	0.875000
39.9	8.3	2.038596	91.5	8.2	0.878251
71.1	14.7	2.026160	155.4	14.0	0.882883
124.2	25.2	1.988406	243.2	21.5	0.866365
		2.012451			**0.879768**

Table B.2 (continued)

> For $Q_t = 4.264$ lt/s

Time (sec)	Increase in Pool 1 (cm)	Q_i (lt/s)	Time (sec)	Increase in Bypass Pool (cm)	Q_b (lt/s)
6.2	2.0	3.161290	12.9	1.5	1.139535
14.2	4.6	3.174648	34.9	4.0	1.123209
25.7	8.3	3.164981	70.0	8.2	1.148000
45.9	14.7	3.138562	120.8	14.0	1.135762
81.8	25.2	3.019071	189.2	21.5	1.113636
		3.131710			**1.132028**

> For $Q_t = 4.623$ lt/s

Time (sec)	Increase in Pool 1 (cm)	Q_i (lt/s)	Time (sec)	Increase in Bypass Pool (cm)	Q_b (lt/s)
5.7	2.0	3.438596	12.5	1.5	1.176000
12.8	4.6	3.521875	32.9	4.0	1.191489
23.8	8.3	3.417647	66.5	8.2	1.208421
42.3	14.7	3.405674	113.7	14.0	1.206684
73.3	25.2	3.369168	178.4	21.5	1.181054
		3.430592			**1.192730**

> For $Q_t = 4.791$ lt/s

Time (sec)	Increase in Pool 1 (cm)	Q_i (lt/s)	Time (sec)	Increase in Bypass Pool (cm)	Q_b (lt/s)
16.7	5.9	3.462275	10.3	1.5	1.427184
28.3	10.5	3.636042	28.1	4.0	1.395018
		3.549159	60.2	8.2	1.334884
			161.0	13.3	0.809565
					1.241663

70

APPENDIX C

DISTANCE BETWEEN GRATES

Table C.1 Discharge values for grates at section (1) and (2)

> For $Q_t = 1.156$ lt/s

Time (sec)	Increase in Pool 1 (cm)	Q_{i1} (lt/s)
41.2	2.0	0.475728
94.7	4.6	0.476030
177.7	8.3	0.457738
313.9	14.7	0.458936
533.8	25.2	0.462645
		0.466215

Time (sec)	Increase in Pool 2 (cm)	Q_{i2} (lt/s)
55.3	2.0	0.354430
137.8	5.0	0.355588
244.6	9.0	0.360589
408.3	15.0	0.360029
		0.357659

Time (sec)	Increase in Bypass Pool (cm)	Q_b (lt/s)
45.1	1.5	0.325942
118.9	4.0	0.329689
236.9	8.2	0.339215
406.5	14.0	0.337515
634.7	21.5	0.331968
		0.000332866

	Grate at section (1)	Grate at section (2)
Efficiency (%)	40.30	30.92

Table C.1 (continued)

> For $Q_t = 1.580$ lt/s

Time (sec)	Increase in Pool 1 (cm)	Q_{i1} (lt/s)
33.4	2.0	0.586826
74.6	4.6	0.604290
134.9	8.3	0.602965
237.2	14.7	0.607336
418.5	25.2	0.590108
		0.598305

Time (sec)	Increase in Pool 2 (cm)	Q_{i2} (lt/s)
35.0	2.0	0.560000
88.0	5.0	0.556818
161.0	9.0	0.547826
267.1	15.0	0.550356
		0.553750

Time (sec)	Increase in Bypass Pool (cm)	Q_b (lt/s)
34.0	1.5	0.432353
92.1	4.0	0.425624
185.7	8.2	0.432741
319.5	14.0	0.429421
499.1	21.5	0.422160
		0.428460

	Grate at section (1)	Grate at section (2)
Efficiency (%)	37.85	35.04

Table C.1 (continued)

> For $Q_t = 2.291$ lt/s

Time (sec)	Increase in Pool 1 (cm)	Q_{i1} (lt/s)
22.7	2.0	0.863436
51.7	4.6	0.871954
93.4	8.3	0.870878
164.2	14.7	0.877345
288.1	25.2	0.857202
		0.868163

Time (sec)	Increase in Pool 2 (cm)	Q_{i2} (lt/s)
23.8	2.0	0.823529
57.1	5.0	0.858144
103.7	9.0	0.850530
170.6	15.0	0.861665
		0.848467

Time (sec)	Increase in Bypass Pool (cm)	Q_b (lt/s)
25.3	1.5	0.581028
68.7	4.0	0.570597
138.7	8.2	0.579380
237.4	14.0	0.577928
372.8	21.5	0.565182
		0.574823

	Grate at section (1)	Grate at section (2)
Efficiency (%)	37.89	37.03

73

Table C.1 (continued)

> For $Q_t = 3.488$ lt/s

Time (sec)	Increase in Pool 1 (cm)	Q_{i1} (lt/s)
16.0	2.0	1.225000
35.2	4.6	1.280682
62.3	8.3	1.305618
108.5	14.7	1.327742
187.4	25.2	1.317823
		1.291373

Time (sec)	Increase in Pool 2 (cm)	Q_{i2} (lt/s)
15.2	2.0	1.289474
34.3	5.0	1.428571
62.1	9.0	1.420290
101.2	15.0	1.452569
		1.397726

Time (sec)	Increase in Bypass Pool (cm)	Q_b (lt/s)
18.4	1.5	0.798913
49.3	4.0	0.795132
99.7	8.2	0.806018
170.1	14.0	0.806584
266.5	21.5	0.790619
		0.799453

	Grate at section (1)	Grate at section (2)
Efficiency (%)	37.02	40.07

Table C.1 (continued)

> For $Q_t = 4.741$ lt/s

Time (sec)	Increase in Pool 1 (cm)	Q_{i1} (lt/s)
10.5	2.0	1.866667
25.8	4.6	1.747287
46.6	8.3	1.745494
82.2	14.7	1.752555
145.0	25.2	1.703172
		1.763035

Time (sec)	Increase in Pool 2 (cm)	Q_{i2} (lt/s)
9.7	2.0	2.020619
25.0	5.0	1.960000
44.9	9.0	1.964365
74.3	15.0	1.978466
		1.980862

Time (sec)	Increase in Bypass Pool (cm)	Q_b (lt/s)
14.5	1.5	1.013793
39.7	4.0	0.987406
80.3	8.2	1.000747
137.1	14.0	1.000729
214.7	21.5	0.981369
		0.996809

	Grate at section (1)	Grate at section (2)
Efficiency (%)	37.19	41.78

Table C.1 (continued)

> For $Q_t = 5.092$ lt/s

Time (sec)	Increase in Pool 1 (cm)	Q_{i1} (lt/s)
9.8	2.0	2.000000
22.9	4.6	1.968559
42.2	8.3	1.927488
75.1	14.7	1.918242
132.5	25.2	1.863849
		1.935628

Time (sec)	Increase in Pool 2 (cm)	Q_{i2} (lt/s)
9.5	2.0	2.063158
23.7	5.0	2.067511
42.1	9.0	2.095012
69.7	15.0	2.109039
		2.083680

Time (sec)	Increase in Bypass Pool (cm)	Q_b (lt/s)
13.5	1.5	1.088889
36.6	4.0	1.071038
74.5	8.2	1.078658
128.3	14.0	1.069369
199.9	21.5	1.054027
		1.072396

	Grate at section (1)	Grate at section (2)
Efficiency (%)	38.02	40.92

Table C.1 (continued)

> For $Q_t = 5.156$ lt/s

Time (sec)	Increase in Pool 1 (cm)	Q_{i1} (lt/s)
9.8	2.0	2.000000
23.4	4.6	1.926496
41.7	8.3	1.950600
74.2	14.7	1.941509
129.7	25.2	1.904086
		1.944538

Time (sec)	Increase in Pool 2 (cm)	Q_{i2} (lt/s)
10.0	2.0	1.960000
23.7	5.0	2.067511
40.6	9.0	2.172414
66.6	15.0	2.207207
		2.101783

Time (sec)	Increase in Bypass Pool (cm)	Q_b (lt/s)
13.0	1.5	1.130769
35.2	4.0	1.113636
72.3	8.2	1.111480
124.0	14.0	1.106452
193.7	21.5	1.087765
		1.110020

	Grate at section (1)	Grate at section (2)
Efficiency (%)	37.71	40.76

Table C.2 Discharge values for grates at section (1) and (3)

> For $Q_t = 1.201$ lt/s

Time (sec)	Increase in Pool 1 (cm)	Q_{i1} (lt/s)
33.1	2.0	0.592145
76.5	4.6	0.589281
137.7	8.3	0.590704
241.4	14.7	0.596769
422.7	25.2	0.584244
		0.590629

Time (sec)	Increase in Pool 3 (cm)	Q_{i3} (lt/s)
82.2	2.0	0.238443
218.9	5.0	0.223847
437.7	10.1	0.226137
747.3	17.1	0.224247
		0.228168

Time (sec)	Increase in Bypass Pool (cm)	Q_b (lt/s)
39.8	1.5	0.369347
101.5	4.0	0.386207
207.0	8.2	0.388213
355.1	14.0	0.386370
556.7	21.5	0.378480
		0.381723

	Grate at section (1)	Grate at section (3)
Efficiency (%)	49.20	19.01

78

Table C.2 (continued)

➢ For $Q_t = 1.426$ lt/s

Time (sec)	Increase in Pool 1 (cm)	Q_{i1} (lt/s)
28.1	2.0	0.697509
66.4	4.6	0.678916
120.5	8.3	0.675021
216.4	14.7	0.665712
370.3	25.2	0.666919
		0.676815

Time (sec)	Increase in Pool 3 (cm)	Q_{i3} (lt/s)
59.9	2.0	0.327212
154.7	5.0	0.316742
309.5	10.1	0.319806
525.5	17.1	0.318896
		0.320664

Time (sec)	Increase in Bypass Pool (cm)	Q_b (lt/s)
34.6	1.5	0.424855
90.7	4.0	0.432194
186.0	8.2	0.432043
318.5	14.0	0.430769
497.6	21.5	0.423432
		0.428659

	Grate at section (1)	Grate at section (2)
Efficiency (%)	47.46	22.48

Table C.2 (continued)

> For $Q_t = 1.625$ lt/s

Time (sec)	Increase in Pool 1 (cm)	Q_{i1} (lt/s)
26.6	2.0	0.736842
60.8	4.6	0.741447
109.6	8.3	0.742153
193.4	14.7	0.744881
338.6	25.2	0.729356
		0.738936

Time (sec)	Increase in Pool 3 (cm)	Q_{i3} (lt/s)
46.8	2.0	0.418803
119.9	5.0	0.408674
239.8	10.1	0.412761
410.2	17.1	0.408532
		0.412193

Time (sec)	Increase in Bypass Pool (cm)	Q_b (lt/s)
30.3	1.5	0.485149
82.8	4.0	0.473430
167.5	8.2	0.479761
292.0	14.0	0.469863
455.9	21.5	0.462163
		0.474073

	Grate at section (1)	Grate at section (2)
Efficiency (%)	45.47	25.36

Table C.2 (continued)

> For Q_t = 1.825 lt/s

Time (sec)	Increase in Pool 1 (cm)	Q_{i1} (lt/s)
22.7	2.0	0.863436
54.0	4.6	0.834815
98.3	8.3	0.827467
174.7	14.7	0.824614
304.8	25.2	0.810236
		0.832114

Time (sec)	Increase in Pool 3 (cm)	Q_{i3} (lt/s)
39.3	2.0	0.498728
101.9	5.0	0.480864
203.7	10.1	0.485911
346.1	17.1	0.484195
		0.487424

Time (sec)	Increase in Bypass Pool (cm)	Q_b (lt/s)
29.2	1.5	0.503425
77.1	4.0	0.508431
158.6	8.2	0.506683
268.8	14.0	0.510417
422.4	21.5	0.498816
		0.505554

	Grate at section (1)	Grate at section (2)
Efficiency (%)	45.59	26.71

APPENDIX D

FLOW DEPTH

Table D.1 Flow depth values (y) for 2 cm gap – 2 cm full system

Q_t (lt/s)	y (cm)
1.830707	1.40
1.880585	1.40
3.639531	1.85
3.756819	1.90
4.514077	2.00

Table D.2 Flow depth values (y) for 2.5 cm gap – 2 cm full system

Q_t (lt/s)	y (cm)
1.552493	1.30
2.252489	1.60
3.603167	1.90
5.205827	2.30

Table D.3 Flow depth values (y) for 2 cm gap – 1.5 cm full system

Q_t (lt/s)	y (cm)
3.579318	1.90
4.034166	2.05
4.45443	2.20
4.983769	2.20

Table D.4 Flow depth values (y) for 2.5 cm gap – 1.5 cm full system

Q_t (lt/s)	y (cm)
1.548387	1.40
2.157820	1.60
3.486761	1.90
4.759055	2.30
5.157464	2.35

Table D.5 Flow depth values (y) for 2 cm gap – 1 cm full system

Q_t (lt/s)	y (cm)
2.215948	1.60
3.535106	1.90
5.104088	2.30
5.236759	2.35
5.565479	2.40
5.272104	2.40

Table D.6 Flow depth values (y) for 2.5 cm gap – 1 cm full system

Q_t (lt/s)	y (cm)
2.112716	1.60
3.529954	1.90
4.847560	2.25
5.026564	2.30
5.047238	2.35